Yang, S., Schulz, H.-M. (2019): Factors controlling the petroleum generation characteristics of Palaeogene source rocks in the Austrian Molasse Basin as revealed by principal component analysis biplots. - *Marine and Petroleum Geology*, *99*, pp. 323—336.

DOI: http://doi.org/10.1016/j.marpetgeo.2018.10.024

Accepted Manuscript

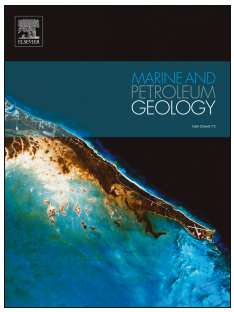

Factors controlling the petroleum generation characteristics of Palaeogene source rocks in the Austrian Molasse Basin as revealed by principal component analysis biplots

Shengyu Yang, Hans-Martin Schulz

PII: S0264-8172(18)30430-6

DOI: 10.1016/j.marpetgeo.2018.10.024

Reference: JMPG 3536

To appear in: *Marine and Petroleum Geology*

Received Date: 18 June 2018

Revised Date: 8 October 2018

Accepted Date: 15 October 2018

Please cite this article as: Yang, S., Schulz, H.-M., Factors controlling the petroleum generation characteristics of Palaeogene source rocks in the Austrian Molasse Basin as revealed by principal component analysis biplots, *Marine and Petroleum Geology* (2018), doi: https://doi.org/10.1016/j.marpetgeo.2018.10.024.

Factors controlling the petroleum generation characteristics of Palaeogene source rocks in the Austrian Molasse Basin as revealed by principal component analysis biplots

Shengyu Yang, Hans-Martin Schulz

Helmholtz Centre Potsdam GFZ - German Research Centre for Geosciences, Department of Geochemistry, Section 3.2 Organic Geochemistry, Telegrafenberg, D-14473 Potsdam, Germany

Keywords: Molasse Basin; biomarker; kinetics; PCA

Abstract

After Rock-Eval & TOC screening and heterogeneity evaluation on 91 Palaeogene source rock samples from a well drilled in the Austrian Molasse Basin, ten shale samples were selected for detailed investigations by means of pyrolysis-gas chromatography, bulk kinetics and biomarker identification and quantification. Afterwards, 2-D biplots based on principal component analysis were applied to unravel the palaeo-environmental control on the development of petroleum source rocks.

All samples are immature source rocks with good petroleum generation potentials. The redox environment during deposition was generally reducing, and palaeosalinity is suggested to be the main factor causing the differences in organic carbon contents among the samples. The hydrogen index values, the gas generation preferences and the aromaticity of the products are controlled by both depositional environment and precursors, and the product of a salinity indicator (MTTC) and the oleanane index is introduced as predictive proxy to evaluate these features. The maturity indicator (Tmax) is revealed as dominated by the stability of the kerogen structure which is controlled by the proportion of organic sulphur compounds in the kerogen. The global Eocene-Oligocene climate change from a greenhouse to an icehouse world is suggested to play an important role in changing the palaeoenvironment and further in influencing the development of petroleum source rocks by triggering upwelling, increasing the palaeo-sea water salinity and decreasing the deposition of carbonate-minerals.

The chemometric method suggested here acts as a powerful tool in identifying the controlling factors for the petroleum generation potential among many variables, and can be applied more widely in petroleum geology when multi-parameters are involved to get quick and meaningful correlations.

Introduction

Chemometrics, which is a conceptual approach of processing data with various numerical techniques in order to extract useful information (Kramer, 1998), plays a very important role in geosciences (Hammer et al., 2001). However, the application of chemometric tools, e.g., hierarchical cluster analysis (HCA) or principal component analysis (PCA), in petroleum geology is generally applied in oil-source rock or oil-oil correlation studies (Peters et al., 2007; Peters et al., 2016; Yang et al., 2017). These powerful statistical approaches can not only group samples with similar geological features but also show the correlations of parameters that differentiate the samples. Therefore, there is also a great potential for chemometrics in unravelling the controlling factors for the development of different petroleum generation characteristics when according parameters are used in the analysis.

The Eocene-Oligocene Schöneck Formation and the overlying Dynow Formation in the Molasse Basin are organic-rich marine deposits with some brackish intervals in the uppermost Schöneck Formation and the Dynow Formation. These source rocks are immature toward the Bohemian Massif direction and enter the oil window at ca. 4 km depth beneath the Alpine nappes (Gratzer et al., 2011). They are considered as the main source rocks for a series of oil fields (Gratzer et al., 2011; Véron, 2005) and thermogenic/biogenic gas reservoirs (Pytlak et al., 2016) found in Upper Austria. Previous work on these Palaeogene source rocks in the Molasse Basin has been focused on palaeoceanography (Schulz et al., 2002), spatial architecture (Sachsenhofer and Schulz, 2006), oil-source rock correlation (Gratzer et al., 2011), and basin modelling (Gusterhuber et al., 2014). However, the vertical heterogeneity of the detailed petroleum generation potential has not been systematically investigated yet. For example, there is still a need to gain compositional information of the hydrocarbon potential which is critically important in predicting the physical properties of producing oil (di Primio and Horsfield, 2006) and the bulk kinetic features which play important roles in determining the timing of petroleum generation during basin modelling (Ungerer and Pelet, 1987). In addition, the determination of the geological controls on these petroleum generation characteristics would improve the understanding of the regional petroleum geology and thus provide implications in finding more effective source rocks in similar geological environments.

Geological background and samples

The Molasse Basin, which is alternatively termed as Alpine Foreland Basin (Crampton and Allen, 1995; Pfiffner, 1986), extends along the northern margin of the Alps from France to the eastern border of Austria (Figure 1). This Cenozoic foreland basin is formed from the subduction of the southern

margin of the European plate beneath the Adriatic plate (Ziegler and Roure, 1999) and is about 900 km long and up to 120 km wide in the German sector in its present-day configuration (Véron, 2005).

The Eocene-Oligocene Schöneck Formation and the Oligocene Dynow Formation consisting of marlstone, shale and thin carbonates (Figure 2) were deposited in a marine to brackish environment. The lithological transition was suggested to be induced by the basin subsidence/uplift and water level changes (Báldi, 1984) which is similar to the depositional model in the Black Sea since 7,500 years bp (Schulz et al., 2005). The sedimentary succession of the Schöneck and Dynow Formations is regional expression of a wider phenomenon and similar palaeo-environmental signals were stored in the rocks developed in the Paratethys realm. For examples, high total organic carbon (TOC) contents can be traced further to the Eastern Paratethys domain where the contemporaneously deposited Maikop Formation is one of the main source rocks for hydrocarbons found in the South Caspian Basin, the Caucasus region, and the Black Sea Basin (Abrams and Narimanov, 1997; Gürgey, 2003; Sachsenhofer et al., 2017).

An available data set (Schulz et al., 2002) was completed by additional core samples to gain a data base of 91 samples from the borehole Oberschauersberg 1 (Osch-1) (Figure 1) with TOC and Rock-Eval data. In the following, ten samples were selected as key representatives of different facies for detailed investigations (Figure 2). Previous investigations focussed on lithology, stratigraphy, and isotopes of this well (Schulz, 2003). The lower part of Schöneck Formation is mainly composed of marlstone with very thin dolomite and volcanic ashes interlayers (Schulz, 2003), while the upper part is featured by carbonate-free claystone with two marlstone interlayers (Figure 2). Three depositional cycles were identified in the overlying Dynow Formation (Schulz et al., 2004), two of which are shown in Figure 2, i.e., the two limestone layers interbedded in the marlstone represent the deposition during highstand systems tracts or massive influx of nutrient-loaden freshwater.

Methods

Powdered samples were analysed for total carbon (TC), total organic carbon (after acidification) and total sulphur contents using a Leco CS-225 analyser after acidification to remove carbonate. The differences between TC and TOC is the total inorganic carbon (TIC). Calcite contents were calculated by multiplying 8.33 with TIC (Espitalié et al., 1977). Rock-Eval pyrolysis was performed using Rock-Eval 6 following established procedures (Behar et al., 2001).

Pyrolysis-GC (PyGC) was performed using the Quantum MSSV-2 Thermal Analysis System interfaced with an Agilent GC-6890A. About 10 mg of coarsely crushed reference shale was filled into a small

open glass tube and heated at 300 °C for three minutes to vent the free hydrocarbons. Hydrocarbons generated between 300 to 600 °C were collected and measured. Quantification of individual compounds was conducted by external standardisation with n-butane.

Bulk kinetic parameters were assessed by subjecting samples to open-system, non-isothermal pyrolysis at four different linear heating rates (0.7, 2, 5, 15 °C/min) using a Source Rock Analyser® (SRA) following established procedures (Yang and Horsfield, 2016). The discrete activation-energy distribution optimization with a single variable frequency factor as well as geological extrapolation was carried out using the KINETICS 2000® and KMOD® programs.

Soxhlet extraction was carried out on powdered shale samples for 24 hrs at 50 °C using dichloromethane and methanol mixture (99:1) as solvent. After asphaltene precipitation, the maltenes were separated into aliphatic, aromatic hydrocarbons, and NSO fractions by medium-pressure liquid chromatography (MPLC) fractionation as described by (Radke et al., 1980). Gas chromatography with flame ionization detector (GC-FID) was carried out on the aliphatic hydrocarbon fractions. The instrument was equipped with a HP Ultra 1 capillary column. The oven temperature was programmed from 40 °C to 300 °C with a 5 °C/min heating rate. GC-MS test runs were based on a Trace GC Ultra system coupled to a DSQ mass spectrometer. The GC was equipped with a PTV injection system and a fused silica capillary column, and was heated from 50 °C to 310 °C at a rate of 3 °C/min.

The hierarchical cluster analysis and principal component analysis are carried out with the PAST statistical programme which is designed for geological research (Hammer et al., 2001). All parameters were normalized to the same scale by using the “correlation matrix” option, so that the variations among different parameters are comparable.

Results

Screening data

Rock-Eval and TOC data as fundamental parameters basically provide information about the organic matter richness, quality, and maturity of the potential source rocks (Table 1). Most of the Dynow Formation samples contain TOC contents between 1% and 2% (Figure 2) and can be classified as “Good Source Rock” based on the criteria suggested by Peters and Cassa (1994). The Schöneck Formation samples are featured by much higher organic contents, and the upper part and lower part can be viewed as “Excellent Source Rock” (TOC > 4%) and “Very Good Source Rock” (2% < TOC < 4%),

respectively (Peters and Cassa, 1994). With 300 mg/gTOC < HI < 600 mg/gTOC, most samples contain type II kerogen (Espitalie et al., 1977). The Upper Schöneck Formation has exceptionally high hydrogen index (HI) values compared with the other intervals whereas the lower part of the Schöneck Formation is featured by relatively lower HI values (Figure 2). All samples are characterized by T_{max} values lower than 435 ^{o}C (Figure 2) and are thermally immature. This conclusion is consistent with previous work which suggest the vitrinite reflectance is lower than 0.35% (Schulz et al., 2002). The average T_{max} values show a decrease from the Dynow Formation to the Lower Schöneck Formation. This trend is neither a reflection of the geological burial history which would suggest a higher thermal maturity of older rocks, nor a bitumen suppression on T_{max} which occurs in high TOC or high HI intervals (Snowdon, 1995).

In brief, the Schöneck and Dynow Formations are natural laboratories with considerable immature organic matter. These intervals can be effective petroleum source rocks at suitable maturity, and are characterized by organic geochemical heterogeneities on decimeter scales (Figure 2). Nevertheless, the three rock units can still be differentiated by their featured Rock-Eval and TOC data. This enables the selection of 10 key samples as representatives of the three intervals (Figure 2) to show their individual petroleum generation characteristics depended on their palaeoceanographic history.

Pyrolysis-gas chromatography

The PyGC analysis of source rocks is a technique that provides a quick evaluation of the kerogen structure (Dembicki et al., 1983; Van de Meent et al., 1980) and relates the structural information to the potential bulk petroleum composition by means of petroleum type organofacies (Horsfield, 1989).

In the Upper Schöneck samples, both gas and oil (up to C_{26}) compositions can be identified (Figure 3B). In comparison, high molecular hydrocarbons in the Dynow Formation and Lower Schöneck Formation are less abundant (Figure 3A and C). Therefore, the petroleum that can be generated in these intervals is predicted as Paraffinic-Naphthenic-Aromatic Oil with low wax content, while the Upper Schöneck samples may generate oil with high wax contents (Figure 4A). When the gas chromatographic signals between C_8 and C_{10} are focused (Figure 3), the Upper Schöneck samples are featured by relatively low concentrations of aromatic compounds compared with neighbouring aliphatic hydrocarbons, while the Lower Schöneck samples generate much higher thiophenic compounds than the rest two intervals. These features become obvious in Figure 4B where diagnostic compounds are used as end members in the ternary diagram. Although, kerogen from all samples can be viewed as type II, the differences in aromaticity and sulphur content of each layer can be clearly identified.

Bulk kinetics

The average activation energy distribution and frequency factors of the Lower Schöneck samples are lower and smaller than the other two intervals (Figure 5). In addition, the peak activation energy of Lower Schöneck Formation is lower than the Upper Schöneck Formation which may indicate a more heterogeneous kerogen structure. The geological extrapolation provides a more direct comparison between the samples (Figure 5). The Lower Schöneck Formation is thus predicted to generate hydrocarbons at much lower temperature than the other two intervals, and the differences in kerogen kinetic stability can also be identified by the geological T_{max} values (Table 1) which were achieved by differentiating the geological transformation curves in Figure 5.

Biomarkers

The pristane/phytane ratios (Pr/Ph) of all samples are in the range of 1.1 - 3.0 (Table 1) which generally imply that they were neither deposited in extremely reducing nor very oxidizing environments. However, inferences from Pr/Ph on redox environment or palaeosalinity should be supported by other geochemical data (Peters et al., 1999).

C_{25} highly branched isoprenoids (C_{25}HBI), which are sourced from benthic (Volkman et al., 1994) or planktonic diatoms (Belt et al., 2001), can be identified in the Schöneck Formation (Figure 6). A relative comparison between the C_{25}HBI and the neighbouring *n*-C_{21} alkane manifests that the Upper Schöneck contains much more abundant C_{25}HBI than the lower part (Table 1 and Figure 6). The relative content ratio of steranes/hopanes in the Lower Schöneck Formation is obviously higher than the other two intervals (Table 1 and Figure 6). This would imply that the Lower Schöneck Formation has a higher dominance of eukaryotes (mainly algae and higher plant) over prokaryotes (bacteria) as organic matter input during deposition (Mello et al., 1988).

The distribution of hopanes in the three intervals is different (Figure 7A). The relative contents of C_{35} homohopane and oleanane decrease from the Lower Schöneck Formation up to the Dynow Formation. Accordingly, the 17α-diahopane which is normally correlated with oleanane (Li et al., 2009) is enriched only in the lower part of the Schöneck Formation (Figure 7A). In addition, unsaturated biomarkers, e.g., norneohop-13(18)-ene and olean-13(18)-ene, can be identified based on retention times and fragment mass information (Curiale and Bromley, 1996; Sinninghe Damsté et al., 2014). The concentrations of tricyclic terpanes are generally low in all samples, because they are not readily released from the kerogen at this level of maturity (Seifert and Moldowan, 1978).

The C_{27}-C_{30} steranes are dominated by ααR isomers (Figure 7B) due to the low organic matter maturity (McKenzie et al., 1983). Obviously, the relative contents of C_{27} and C_{30} steranes in the Dynow Formation are much lower than in the other intervals and indicate a shallower marine environment than during deposition of the Schöneck Formation (Figure 8).

In the aromatic fraction of biomarkers, four alkylated methyl-trimethyl-tridecyl-chromans (MTTCs), which are derived from eu-bacteria and archaea (Damsté et al., 1987) or are formed via the condensation of chlorophyll and alkylphenols (Li et al., 1995), can be detected in the Schöneck Formation (Figure 9). The distributions of the methylated MTTCs indicate salinity changes of the surface water of a density stratified water column, i.e. the value of MTTC ratio (defined as trimethyl-MTTC/sum of the four alkylated MTTC) is negatively correlated with palaeosalinity (Sinninghe Damsté et al., 1993). By the absence of 8-methyl-MTTC, the Dynow Formation samples have higher MTTC ratios than Schöneck Formation (Figure 9). Within the Schöneck Formation, the upper part has less profound dominance of trimethyl-MTTC which implies a high palaeosalinity.

Discussion

Chemometric analyses

To elucidate the controlling factors for the different petroleum generation features of the three intervals, diagnostic geochemical parameters (listed in Table 1) were used to carry out the chemometric analyses. The general result is that the three source rocks can be clearly separated from each other in the HCA (Figure 10A) and PCA (Figure 10B). More importantly, the biplots which demonstrate how the samples are differentiated from each other show correlations between screening parameters (Rock-Eval, TOC and sulphur content), pyrolytic features (PyGC and bulk kinetics), and biomarkers (Figure 10B). It needs to be noticed that a certain percentage of interpreted total variance by PC1 and PC2 is required for a reliable interpretation of the biplots (an empirical minimum lower limit for this is suggested to be 80% here).

It can be observed that the Lower Schöneck Formation is different from the other two intervals by very low T_{max} values whereas the Upper Schöneck Formation is featured by high TOC contents and HI values (Figure 10B) which are consistent with Figure 2. In 2-dimensional PCA biplots, the lengths of the vectors estimate the standard deviations of the respective variables and the cosine values of angles between vectors approximate the intervariable correlations (Aitchison and Greenacre, 2002). In other words, parameter vectors at 0^{o} or 180^{o} angles are highly correlated (either positively or

negatively), while those being mutually perpendicular vectors are generally independent from each other.

TOC enrichment

Productivity (Pedersen and Calvert, 1990; Totman Parrish and Curtis, 1982), preservation (Demaison, 1991; Demaison and Moore, 1980), and sedimentation rate (Creaney and Passey, 1993; Ibach, 1982) are typically considered as the most important factors controlling the organic matter richness in petroleum source rocks (Littke et al., 1997). Many examples demonstrate that one factor alone is generally insufficient to yield organic carbon-rich and oil-prone sediments (Katz, 2005), and the thresholds of the aforementioned factors in the investigated samples thus have to be reached. The vectors of TOC and MTTC ratios are roughly at 175^{o} (Figure 10B) which implies a negative correlation between these two parameters, and this can be confirmed by Figure 11A. Therefore, samples with high TOC contents are associated with a high salinity depositional environment (MTTC ratio inversely correlates with palaeosalinity). In addition, the generally negative correlation between TOC contents and Pr/Ph ratios (Figure 11B) is reflected by the wide angle between these two vectors (Figure 10B). It seems that Pr/Ph of the investigated samples is a reflection of palaeosalinity (ten Haven et al., 1987) and associated redox conditions in the bottom water (Didyk et al., 1978). The salinity influence on TOC enrichment is also supported by previous research, e.g., the TOC contents of the Laney member of the Green River Shale which was deposited in alkaline water is significantly higher than in the freshwater deposits of the Luman Tongue Green River shale (Horsfield et al., 1994).

The difference in palaeosalinity is perhaps a comprehensive representative of the variations in productivity, redox environment, and sedimentation rate to some degree. Marine environments with low salinity (brackish water) are normally influenced by freshwater fluxes from the landside. Depending on the intensity of the flux, a variability of salinity gradients will be induced. For the depositional time slice of the Lower Schöneck Formation, bottom water anoxia was probably induced by salinity stratification. However, at the same time the supply of the re-mineralized nutrients to the sea surface, particularly nitrate and phosphate in dissolved form, would have been strongly hindered by the halocline (Widayat et al., 2016), and thus the primary productivity also decreased significantly. When it came to the deposition of Upper Schöneck Formation, the Paratethys started isolating from the Tethys Ocean in response of the strong tectonic activity and a small but constrained basin was formed (Báldi, 1984). Contemporaneously, the Eocene-Oligocene glaciation caused a temperature drop (ca. 11 ^{o}C), whereas humidity, stratification, bottom water anoxia, and salinity increased within the Paratethys realm (Sotak, 2010; van der Boon et al., 2018). This multifactorial scenario set the scene to enable the deposition of Upper Schöneck Formation with favourable conditions for the

preservation of sediments with high TOC contents. In the case of the Dynow Formation, much more fresh water was induced to the shelf regions, and thus the formerly prevailing water stratification and anoxia collapsed. The less reducing environment coupled to high sedimentation rates led to less organic matter preservation due to oxidation and dilution.

It is important to note that a correlation between salinity and organic matter enrichment may exist if only the depositional environment is generally reducing and when a certain level of productivity is reached, otherwise the salinity could be a minor factor. Also, extremely high salinity environments are not *per se* suitable depositional realms for the deposition of successful petroleum source rock, e.g., evaporites which are typically deposited in hypersaline environment can be featured by low organic carbon contents and very low pyrolysis yields (Katz et al., 1987).

Hydrocarbon generation potential

The HI and the composition of pyrolysates together define the quantity and quality of the hydrocarbons that can be generated from the source rock. The negative correlations between the HI values and the gaseous and aromatic compounds generated in PyGC (Figure 10B and 12A) are consistent with previous findings (Mahlstedt, 2012; Yang and Horsfield, 2016) and reflect the structural features of the kerogen. It seems that there is no single palaeoenvironmental parameter which directly controls the HI values and the pyrolysate composition. However, the oleanane index (OL index) and the MTTC ratio may both affect these quality indicators as suggested by the biplots (Figure 10B). Considered as an indicator of flower plants (Moldowan et al., 1994), the OL index reflects the influence of such precursors on the hydrocarbon generation potential, i.e., a higher input of terrestrial advanced plants may decrease the HI (Figure 12B). The general correlation between salinity and HI (Figure 12C) is linked with the environment during the process of selective preservation of the organic matter in forming kerogen (Tegelaar et al., 1989). Intense reworking of liptinite can take place in aquatic sedimentary systems and bacterial material can be added to the organic matter, and thus a higher ratio of vitrinite (leading to low HI) can be preserved (Vandenbroucke and Largeau, 2007).

The vectors of the OL index and MTTC plot at similar angles with HI, but toward very different directions (Figure 10B). Therefore, the combination of these two parameters can compensate their respective deviations from HI and provides a much higher correlation (Figure 12D). The OL index*MTTC suggested here takes both precursor and depositional environment into account in evaluating the controlling factors of hydrocarbon generation potential, and can be applied in other study areas with similar geological situations.

Controls on maturity

The maturity indictor T_{max} is obviously controlled by kinetic features of the kerogen (GeoTmax) (Figure 10B and 13A). At the same time, the kinetic stability of the kerogen is highly correlated with the relative content of 2, 3-dimethylthiophene generated via pyrolysis (Figure 13B) which is a reflection of the abundance of organic sulphur (Eglinton et al., 1990). The sulphur content of the sediments occurs as inorganic bound sulphur (e.g. in pyrite) and as organic sulphur, which was incorporated into the macromolecular sedimentary organic matter from abiogenic sulphur sources during early diagenesis (Morse and Berner, 1995). Organic bound sulphur decreases the kerogen stability because of either the relative weakness of C-S bonds (Orr, 1986) or sulphur radicals which allow the thermal cracking of C-C bonds to occur at a faster rate and lower thermal stress (Lewan, 1998).

In the Molasse Basin, the unique depositional environment of the shaly to marly Lower Schöneck Formation (dysoxic bottom water with sufficient sulphate supply from the surface water by diffusion) led to the organic sulphur enrichment. These compounds caused the pyrolysates to be rich in alkylated thiophenes lowering the kinetic stability of the kerogen and thus decreasing the T_{max} values. In comparison, more ferric iron was available by continental run-off during the deposition of Upper Schöneck Formation (Schulz et al., 2002). In the anoxic bottom water, sulphate was reduced to sulfide and was bounded in pyrite as inorganic sulphur rather than in kerogen as organic sulphur.

Possible impact from climate change at the E/O boundary

The Upper Schöneck Formation which possesses the best petroleum generation potential was generally developed after the initiation of the Antarctic glaciation around the Eocene-Oligocene boundary which caused a global change from a greenhouse to an icehouse world (Savin et al., 1975; van der Boon et al., 2018). Recent palaeoceanographic research on the $\delta^{18}O$ and $\delta^{13}C$ data of foraminifera reveals that the globally established temperature change trend across the E/O boundary can also be recognized in the Paratethys realm (Ozsvart et al., 2016). Besides the local tectonic movements and sea level change, the impact of glaciation-induced cooling on the deposition of the petroleum source rock in the Molasse Basin should be highlighted (Parrish, 1982).

Upwelling phenomena may be triggered during glacial periods because of a combination of stronger and more persistent winds, more extreme thermal gradients, and intensified oceanic circulation patterns (Kennett, 1982). Within the Paratethys, upwelling was suggested to be contemporaneously developed with the E/O boundary glaciation by previous studies (Gier, 2000; Vetö, 1987; Wagner,

1998). It was also reported that the upwelling off northern California (Sancetta et al., 1992) and off eastern New Zealand (Nelson et al., 2000) have both been enhanced by the last glaciation. When the investigated Upper Schöneck Formation was deposited, the shoreline lay in the north (Schulz et al., 2004) and the nearshore wind came from the west and paralleled the coast (von der Heydt and Dijkstra, 2006). These factors meet the prerequisites for the initiation of a wind-driven upwelling system (Sarhan, 2000). This hypothesis is supported by the high concentration of C_{25} HBI in Upper Schöneck Formation (Figure 6) which denotes a diatom flourishing (Belt et al., 2001) and can be typically observed in the modern Peru upwelling (Volkman et al., 1981) and the Arabian Sea upwelling regions (Wakeham et al., 2002). Sedimentological research revealed that the Upper Schöneck Formation investigated here (well Osch-1) locates in a slope facies during deposition and it contains much higher TOC content (3-11%) compared with its counterpart layer in a basin floor facies (0.4% < TOC < 2.5%) which was presented in well Obhf-1 by Schulz et al. (2002). The differences in TOC contents are not caused by maturation, as the Schöneck Formation in well Obhf-1 is at early oil window maturity (Ro = 0.51 - 0.59%; Schulz et al. 2002) and the TOC consumption on such marine shale is anticipated to be very limited (at maximum 1%) at this stage of maturity (Jarvie, 2012). In contrast, it is more likely that the upwelling brought dissolved nutrients from deep and cold bottom water to only the coastal area and led to a significant biota (e.g., diatoms) flourishing and an expansion of the oxygen minimum zone near the shoreline. As a result, organic matter with higher HI values has been preferentially preserved in the investigated proximal Upper Schöneck Formation compared with deeper facies. In addition, the sedimentation rate in an upwelling system is typically higher in a coastal-parallel ribbon than in a nearby or outer facies (Suess et al., 1987). Such a spatial black shale architecture has been demonstrated for the Upper Schöneck Formation which reaches its maximum thickness in a narrow belt parallel to the palaeo-shoreline (Sachsenhofer and Schulz, 2006).

Besides the described upwelling hypothesis, an increase in global sea water salinity and a decreased carbonate mineral deposition can also be induced by the global cooling event and can further influence the development of petroleum source rocks. Pore fluid measurement of the chloride concentrations and oxygen isotopic compositions of Ocean Drilling Program cores revealed that the deep ocean water salinity was obviously enhanced in response of Last Glacial Maximum (Adkins et al., 2002), because significant amount of freshwater was trapped in the polar ice sheet. A recent study revealed that the reduced atmospheric temperature is also responsible for the enhanced ocean stratification in the North Atlantic during the last glacial maximum (Jansen, 2017). The increased salinity and water stratification thus favour organic matter preservation. The global temperature drop in sea water would also increase the $CaCO_3$ dissolution, and thus decrease the proportion of

carbonate minerals in the deposits. For example, geological records manifest that the CCD in the Pacific Ocean was deepened for more than 1 km near the Eocene/Oligocene boundary (Coxall et al., 2005). In the case of the Molasse Basin, the water depth during the deposition of the Schöneck Formation was between 400 – 800 m (Dohmann, 1991) which is far shallower than the average CCD (3.5 – 4.5 km) (Bickert, 2009). Nevertheless, the transition from the Lower Schöneck marlstone to the Upper Schöneck carbonate-free shale, which typically contains higher organic matter than marlstone, might be influenced by the temperature change in addition to the water level fluctuation. It needs to be pointed out that the development of the Upper Schöneck Formation does not exactly coincide with the E/O boundary (Figure 2). This is caused by the delayed response of the sedimentary record from the global temperature change which can also observed in central North America (Zanazzi et al., 2007) and in the Central-Carpathian Paleogene Basin (Sotak, 2010) during the E/O transition. Contemporaneously deposited with the Upper Schöneck Formation, there are many other effective marine source rocks developed right after the Antarctic glaciation all around the world, e.g., the Jenam formation in Surma Basin (Bangladesh) (Curiale et al., 2002), the Shahejie formation in Bohai Bay Basin (China) (Li et al., 2003), the Heath formation in Talara Basin (Peru) (Fildani et al., 2005), and the Maikop group in Eastern Paratethys realm (Sachsenhofer et al., 2017). These would imply that the correlation between the E/O global cooling event and the development of excellent petroleum source rock is not merely a coincidence in the Molasse Basin, but may exist in a wider area all over the world.

Conclusions

The Schöneck Formation and Dynow Formation are marine to brackish deposits with great petroleum generation potential. With the aid of the PCA based biplots, the systematic differences in TOC, HI, and Tmax are actually controlled by palaeoenvironment and precursor.

The biplots can not only figure out the correlations of two key factors among numerous variables, but also enable to elaborate meaningful parameters which are combined from multi-factors, e.g., MTTC*OL index. The correlative information provided by the biplots enables quick evaluations on how petroleum generation features are controlled by palaeo-environmental factors.

The global cooling event at the E/O boundary might have played a very important role in favouring the development of excellent petroleum source rocks by triggering upwelling, increasing sea-water salinity, and decreasing the carbonate deposition.

Acknowledgement

We thank Ferdinand Perssen, Anke Kaminsky and Cornelia Karger for their technical support. Reviews and constructive comments from two anonymous referees are much appreciated.

Figure and table captions

Figure 1. Geological situation of the Molasse Basin and the location of well Oberschauersberg 1(Osch1).

Figure 2. Simplified stratigraphy of the Schöneck Formation and Dynow Formation in well Oberschauersberg 1. 10 representative samples (circle) were selected to carry out more detailed research based on the Rock-Eval and TOC screening of the 91 samples (rhombus). Sample numbers of the selected samples are listed on the right part of the figure.

Figure 3. PyGC traces of the three source rocks. Aliphatic hydrocarbon doublets are marked by carbon numbers. Aromatic compounds listed in the figures are *meta*-, *para*-xylene, *ortho*-xylene, and 1, 2, 4-Trimethylbenzene, respectively. Thiophenic compounds include, from left to right, 2-Ethylthiophene, 2,5-Dimethylthiophene, 2,4-Dimethylthiophene, 2,3-Dimethylthiophene, and 2-Ethyl-5-Methylthiophene.

Figure 4. Ternary diagrams of the pyrolysates for interpretations of organic facies and kerogen structures of the samples.(A) Petroleum products prediction based on chain-length distribution (Horsfield, 1989) and (B) organic type classification based on diagnostic aliphatic, aromatic, and thiophenic compounds (Eglinton et al., 1990).

Figure 5. The geological extrapolation (heating rate of 3 K/million year) of the bulk kinetic parameters. Three end member samples are shown by detailed activation energy distribution and frequency factors. The yellow dot line depicts the calculated vitrinite reflectance based on EASY%Ro method (Sweeney and Burnham, 1990). The calculated $GeoT_{max}$ for each sample can be found in Table 1.

Figure 6. Total ion chromatogram traces of three end member samples. Saturated hydrocarbons are shown by carbon numbers. Sterane and hopanes are marked by carbon numbers plus “S” and “H”, respectively.

Figure 7. Comparison of hopane (A) and sterane (B) traces of three representative samples. Ts=18α-trisnorneohopane; Tm=17α –trisnorhopane; D30= 17α-diahopane; OL=oleanane. The diamond marked peak in (A) is norneohop-13(18)-ene for Dynow Formation, and it is co-elution of norneohop-13(18)-ene and olean-13(18)-ene for Schöneck samples.

Figure 8. Ternary diagram showing the relative distribution of αααR C_{27}, C_{28}, and C_{29} steranes (Huang and Meinschein, 1979).

Figure 9. Mass chromatograms of m/z 107 + 121 + 135 + 149 revealing the distributions of the methylated MTTCs. I=8-methyl-MTTC; II a=7,8-dimethyl-MTTC; II b=5,8-dimethyl-MTTC; III=5,7,8-trimethyl-MTTC.

Figure 10. Chemometric analysis on the 10 source rock samples (Dy=Dynow, US= Upper Schöneck, and LS=Lower Schöneck). Geochemical parameters used as inputs were listed in Table 1. (A) Three group can be clearly separated from each other by the hierarchical cluster analysis. (B) 2-dimentional principal

component analysis show how the three groups of samples are differentiated from each other and the correlations between screening data (marked in red), pyrolytic data (marked in blue) and biomarkers (marked in green) can be revealed by the biplots. Component 1 and component 2 together have interpreted 83.44% of the variances among the samples.

Figure 11. (A) TOC is negatively proportional to alkylated methyl-trimethyl-tridecyl-chromans (MTTC) ratio. (B) TOC is also generally negatively correlated with pristane over phytane ratio.

Figure 12. Hydrogen index (HI) is highly correlated with the relative percentage of gas in the pyrolysate (A). The correlations of HI vs. oleanane index (B) and HI vs. MTTC (C) are much lower than the correlation of HI vs. the product of MTTC and oleanane index (D).

Table 1. A compilation of geochemical parameters used in the research. The * marked parameters were applied in the chemometric analysis as shown in Figure 10. For PyGC data, the first six columns show the data used in Figure 4 A and B, three for each. $GeoT_{max}$ values were achieved by differentiating the geological transformation curves in Figure 5. For biomarkers, “H” stands for hopanes, “O” represents oleanane, and “St” is short for steranes.

Reference

Abrams, M. A., and A. A. Narimanov, 1997, Geochemical evaluation of hydrocarbons and their potential sources in the western South Caspian depression, Republic of Azerbaijan: Marine and Petroleum Geology, v. 14, p. 451-468.

Adkins, J. F., K. McIntyre, and D. P. Schrag, 2002, The salinity, temperature, and δ18O of the glacial deep ocean: Science, v. 298, p. 1769-1773.

Aitchison, J., and M. Greenacre, 2002, Biplots of compositional data: Journal of the Royal Statistical Society: Series C (Applied Statistics), v. 51, p. 375-392.

Báldi, T., 1984, The terminal Eocene and Early Oligocene events in Hungary and the separation of an anoxic, cold Paratethys: Eclogae Geologicae Helvetiae, v. 77, p. 1-27.

Behar, F., V. Beaumont, and H. L. D. Penteado, 2001, Rock-Eval 6 technology: Performances and developments: Oil & Gas Science and Technology-Revue D Ifp Energies Nouvelles, v. 56, p. 111-134.

Belt, S. T., G. Massé, W. G. Allard, J.-M. Robert, and S. J. Rowland, 2001, C25 highly branched isoprenoid alkenes in planktonic diatoms of the Pleurosigma genus: Organic Geochemistry, v. 32, p. 1271-1275.

Bickert, T., 2009, Carbonate compensation depth, Encyclopedia of Paleoclimatology and Ancient Environments, Springer, p. 136-138.

Coxall, H. K., P. A. Wilson, H. Palike, C. H. Lear, and J. Backman, 2005, Rapid stepwise onset of Antarctic glaciation and deeper calcite compensation in the Pacific Ocean: Nature, v. 433, p. 53-7.

Crampton, S., and P. Allen, 1995, Recognition of forebulge unconformities associated with early stage foreland basin development: example from the North Alpine Foreland Basin: AAPG bulletin, v. 79, p. 1495-1514.

Creaney, S., and Q. R. Passey, 1993, Recurring patterns of total organic carbon and source rock quality within a sequence stratigraphic framework: AAPG Bulletin, v. 77, p. 386-401.

Curiale, J. A., and B. W. Bromley, 1996, Migration of petroleum into Vermilion 14 field, Gulf Coast, USA - Molecular evidence: Organic Geochemistry, v. 24, p. 563-579.

Curiale, J. A., G. H. Covington, A. H. M. Shamsuddin, J. A. Morelos, and A. K. M. Shamsuddin, 2002, Origin of petroleum in Bangladesh: AAPG bulletin, v. 86, p. 625-652.

Damsté, J. S. S., A. C. Kock-Van Dalen, J. W. De Leeuw, P. A. Schenck, S. Guoying, and S. C. Brassell, 1987, The identification of mono-, di- and trimethyl 2-methyl-2-(4,8,12-trimethyltridecyl)chromans and their occurrence in the geosphere: Geochimica et Cosmochimica Acta, v. 51, p. 2393-2400.

Demaison, G., 1991, Anoxia vs. Productivity: What Controls the Formation of Organic-Carbon-Rich Sediments and Sedimentary Rocks?: Discussion (1): AAPG Bulletin, v. 75, p. 499-499.

Demaison, G., and G. T. Moore, 1980, Anoxic environments and oil source bed genesis: Organic Geochemistry, v. 2, p. 9-31.

Dembicki, H., B. Horsfield, and T. T. Ho, 1983, Source rock evaluation by pyrolysis-gas chromatography: AAPG Bulletin, v. 67, p. 1094-1103.

di Primio, R., and B. Horsfield, 2006, From petroleum-type organofacies to hydrocarbon phase prediction: AAPG Bulletin, v. 90, p. 1031-1058.

Didyk, B. M., B. R. T. Simoneit, S. C. Brassell, and G. Eglinton, 1978, Organic geochemical indicators of palaeoenvironmental conditions of sedimentation: Nature, v. 272, p. 216-222.

Dohmann, L., 1991, Die unteroligozänen Fischschiefer im Molassebecken: Inauguraldissertation Univ. München.

Eglinton, T. I., J. S. S. Damste, M. E. L. Kohnen, and J. W. Deleeuw, 1990, Rapid Estimation of the Organic Sulfur-Content of Kerogens, Coals and Asphaltenes by Pyrolysis-Gas Chromatography: Fuel, v. 69, p. 1394-1404.

Espitalié, J., J. L. Laporte, M. Madec, F. Marquis, P. Leplat, J. Paulet, and A. Boutefeu, 1977, Méthode rapide de caractérisation des roches mètres, de leur potentiel pétrolier et de leur degré d'évolution: Revue de l'Institut français du Pétrole, v. 32, p. 23-42.

Espitalie, J., M. Madec, B. Tissot, J. Mennig, and P. Leplat, 1977, Source rock characterization method for petroleum exploration: The 9th Annual Offshore Technology Conference, p. 439-44.

Fildani, A., A. D. Hanson, Z. Chen, J. M. Moldowan, S. A. Graham, and P. R. Arriola, 2005, Geochemical characteristics of oil and source rocks and implications for petroleum systems, Talara basin, northwest Peru: AAPG bulletin, v. 89, p. 1519-1545.

Gier, S., 2000, Clay mineral and organic diagenesis of the Lower Oligocene Scho ¨neck Fishshale, western Austrian Molasse Basin: Clay Minerals, v. 35, p. 709-717.

Gratzer, R., A. Bechtel, R. F. Sachsenhofer, H. G. Linzer, D. Reischenbacher, and H. M. Schulz, 2011, Oil-oil and oil-source rock correlations in the Alpine Foreland Basin of Austria: Insights from biomarker and stable carbon isotope studies: Marine and Petroleum Geology, v. 28, p. 1171-1186.

Gürgey, K., 2003, Correlation, alteration, and origin of hydrocarbons in the GCA, Bahar, and Gum Adasi fields, western South Caspian Basin: geochemical and multivariate statistical assessments: Marine and Petroleum Geology, v. 20, p. 1119-1139.

Gusterhuber, J., R. Hinsch, and R. F. Sachsenhofer, 2014, Evaluation of hydrocarbon generation and migration in the Molasse fold and thrust belt(Central Eastern Alps, Austria) using structural and thermal basin models: AAPG Bulletin, v. 98, p. 253-277.

Hammer, Ø., D. Harper, and P. Ryan, 2001, PAST-Palaeontological statistics, v. 25, p. 2009.

Horsfield, B., 1989, Practical criteria for classifying kerogens: some observations from pyrolysis-gas chromatography: Geochimica et Cosmochimica Acta, v. 53, p. 891-901.

Horsfield, B., D. J. Curry, K. Bohacs, R. Littke, J. Rullkötter, H. J. Schenk, M. Radke, R. G. Schaefer, A. R. Carroll, G. Isaksen, and E. G. Witte, 1994, Organic geochemistry of freshwater and alkaline lacustrine sediments in the Green River Formation of the Washakie Basin, Wyoming, U.S.A: Organic Geochemistry, v. 22, p. 415-440.

Huang, W.-Y., and W. G. Meinschein, 1979, Sterols as ecological indicators: Geochimica et Cosmochimica Acta, v. 43, p. 739-745.

Ibach, L. E. J., 1982, Relationship between sedimentation rate and total organic carbon content in ancient marine sediments: AAPG Bulletin, v. 66, p. 170-188.

Jansen, M. F., 2017, Glacial ocean circulation and stratification explained by reduced atmospheric temperature: Proc Natl Acad Sci U S A, v. 114, p. 45-50.

Jarvie, D. M., 2012, Shale resource systems for oil and gas: Part 1—Shale-gas resource systems: AAPG Memoir, p. 69-87.

Katz, B. J., 2005, Controlling factors on source rock development—a review of productivity, preservation, and sedimentation rate: SEPM Special Publication, v. 82, p. 7–16.

Katz, B. J., K. K. Bissada, and J. W. Wood, 1987, Factors limiting potential of evaporites as hydrocarbon source rocks: 1987 SEG Annual Meeting.

Kennett, J. P., 1982, Marine Geology, 813 pp, Prentice-Hall, Englewood Cliffs, NJ.

Kramer, R., 1998, Chemometric techniques for quantitative analysis, CRC Press.

Lewan, M. D., 1998, Sulphur-radical control on petroleum formation rates: Nature, v. 391, p. 164-166.

Li, M., S. R. Larter, P. Taylor, D. M. Jones, B. Bowler, and M. Bjorøy, 1995, Biomarkers or not biomarkers? A new hypothesis for the origin of pristane involving derivation from methyltrimethyltridecylchromans (MTTCs) formed during diagenesis from chlorophyll and alkylphenols: Organic Geochemistry, v. 23, p. 159-167.

Li, M., T. Wang, J. Liu, M. Zhang, H. Lu, Q. Ma, and L. Gao, 2009, Biomarker 17α(H)-diahopane: A geochemical tool to study the petroleum system of a Tertiary lacustrine basin, Northern South China Sea: Applied Geochemistry, v. 24, p. 172-183.

Li, S. M., X. Q. Pang, M. W. Li, and Z. J. Jin, 2003, Geochemistry of petroleum systems in the Niuzhuang South Slope of Bohai Bay Basin - part 1: source rock characterization: Organic Geochemistry, v. 34, p. 389-412.

Littke, R., D. Baker, and J. Rullkötter, 1997, Deposition of petroleum source rocks, Petroleum and Basin Evolution, Springer, p. 271-333.

Mahlstedt, N. L., 2012, Evaluating the late gas potential of source rocks stemming from different sedimentary environments genehmigte Dissertation, 370pp-370pp p.

McKenzie, D., A. S. Mackenzie, J. R. Maxwell, and C. Sajgo, 1983, Isomerization and aromatization of hydrocarbons in stretched sedimentary basins: Nature, v. 301, p. 504-506.

Mello, M., P. Gaglianone, S. Brassell, and J. Maxwell, 1988, Geochemical and biological marker assessment of depositional environments using Brazilian offshore oils: Marine and petroleum Geology, v. 5, p. 205-223.

Moldowan, J. M., J. Dahl, B. J. Huizinga, F. J. Fago, L. J. Hickey, T. M. Peakman, and D. W. Taylor, 1994, The molecular fossil record of oleanane and its relation to angiosperms: Science, v. 265, p. 768-71.

Morse, J. W., and R. A. Berner, 1995, What determines sedimentary C/S ratios?: Geochimica et Cosmochimica Acta, v. 59, p. 1073-1077.

Nelson, C. S., I. L. Hendy, H. L. Neil, C. H. Hendy, and P. P. E. Weaver, 2000, Last glacial jetting of cold waters through the Subtropical Convergence zone in the Southwest Pacific off eastern New Zealand, and some geological implications: Palaeogeography, Palaeoclimatology, Palaeoecology, v. 156, p. 103-121.

Orr, W. L., 1986, Kerogen/asphaltene/sulfur relationships in sulfur-rich Monterey oils: Organic Geochemistry, v. 10, p. 499-516.

Ozsvart, P., L. Kocsis, A. Nyerges, O. Gyori, and J. Palfy, 2016, The Eocene-Oligocene climate transition in the Central Paratethys: Palaeogeography Palaeoclimatology Palaeoecology, v. 459, p. 471-487.

Parrish, J. T., 1982, Upwelling and petroleum source beds, with reference to Paleozoic: AAPG Bulletin, v. 66, p. 750-774.

Pedersen, T., and S. Calvert, 1990, Anoxia vs. productivity: what controls the formation of organic-carbon-rich sediments and sedimentary Rocks?(1): AAPG Bulletin, v. 74, p. 454-466.

Peters, K. E., and M. R. Cassa, 1994, Applied source rock geochemistry, *in* L. B. Magoon, and W. G. Dow, eds., The Petroleum System--From Source to Trap: AAPG Memoirs, American Association of Petroleum Geologists, p. 93-120.

Peters, K. E., T. H. Fraser, W. Amris, B. Rustanto, and E. Hermanto, 1999, Geochemistry of crude oils from eastern Indonesia: AAPG Bulletin, v. 83, p. 1927-1942.

Peters, K. E., L. S. Ramos, J. E. Zumberge, Z. C. Valin, C. R. Scotese, and D. L. Gautier, 2007, Circum-Arctic petroleum systems identified using decision-tree chemometrics: AAPG Bulletin, v. 91, p. 877-913.

Peters, K. E., T. L. Wright, L. S. Ramos, J. E. Zumberge, and L. B. Magoon, 2016, Chemometric recognition of genetically distinct oil families in the Los Angeles basin, California: AAPG Bulletin, v. 100, p. 115-135.

Pfiffner, O. A., 1986, Evolution of the north Alpine foreland basin in the Central Alps, Wiley Online Library.

Pytlak, L., D. Gross, R. F. Sachsenhofer, A. Bechtel, and H. G. Linzer, 2016, Gas accumulations in Oligocene–Miocene reservoirs in the Alpine Foreland Basin (Austria): evidence for gas mixing and gas degradation: International Journal of Earth Sciences, v. 106, p. 2171-2188.

Radke, M., H. Willsch, and D. H. Welte, 1980, Preparative hydrocarbon group type determination by automated medium pressure liquid chromatography: Analytical Chemistry, v. 52, p. 406-411.

Sachsenhofer, R. F., S. V. Popov, M. A. Akhmetiev, A. Bechtel, R. Gratzer, D. Groß, B. Horsfield, A. Rachetti, B. Rupprecht, W. B. H. Schaffar, and N. I. Zaporozhets, 2017, The type section of the Maikop Group (Oligocene–lower Miocene) at the Belaya River (North Caucasus): Depositional environment and hydrocarbon potential: AAPG Bulletin, v. 101, p. 289-319.

Sachsenhofer, R. F., and H. M. Schulz, 2006, Architecture of Lower Oligocene source rocks in the Alpine Foreland Basin: a model for syn- and post-depositional source-rock features in the Paratethyan realm: Petroleum Geoscience, v. 12, p. 363-377.

Sancetta, C., M. Lyle, L. Heusser, R. Zahn, and J. P. Bradbury, 1992, Late-Glacial to Holocene Changes in Winds, Upwelling, and Seasonal Production of the Northern California Current System: Quaternary Research, v. 38, p. 359-370.

Sarhan, T., 2000, Upwelling mechanisms in the northwestern Alboran Sea: Journal of Marine Systems, v. 23, p. 317-331.

Savin, S. M., R. G. Douglas, and F. G. Stehli, 1975, Tertiary marine paleotemperatures: Geological Society of America Bulletin, v. 86, p. 1499.

Schulz, H.-M., 2003, Die westliche Zentral-Paratethys an der Wende Eozän/Oligozän.

Schulz, H.-M., A. Bechtel, and R. Sachsenhofer, 2005, The birth of the Paratethys during the Early Oligocene: From Tethys to an ancient Black Sea analogue?: Global and Planetary Change, v. 49, p. 163-176.

Schulz, H. M., A. Bechtel, T. Rainer, R. F. Sachsenhofer, and U. Struck, 2004, Paleoceanography of the western central Paratethys during early oligocene nannoplankton zone NP23 in the Austrian Molasse Basin: Geologica Carpathica, v. 55, p. 311-323.

Schulz, H. M., R. F. Sachsenhofer, A. Bechtel, H. Polesny, and L. Wagner, 2002, The origin of hydrocarbon source rocks in the Austrian Molasse Basin (Eocene-Oligocene transition): Marine and Petroleum Geology, v. 19, p. 683-709.

Seifert, W. K., and J. M. Moldowan, 1978, Applications of steranes, terpanes and monoaromatics to the maturation, migration and source of crude oils: Geochimica et Cosmochimica Acta, v. 42, p. 77-95.

Sinninghe Damsté, J. S., B. J. Keely, S. E. Betts, M. Baas, J. R. Maxwell, and J. W. de Leeuw, 1993, Variations in abundances and distributions of isoprenoid chromans and long-chain alkylbenzenes in sediments of the Mulhouse Basin: a molecular sedimentary record of palaeosalinity: Organic Geochemistry, v. 20, p. 1201-1215.

Sinninghe Damsté, J. S., S. Schouten, and J. K. Volkman, 2014, C27–C30 neohop-13(18)-enes and their saturated and aromatic derivatives in sediments: Indicators for diagenesis and water column stratification: Geochimica et Cosmochimica Acta, v. 133, p. 402-421.

Snowdon, L. R., 1995, Rock-Eval Tmax suppression: documentation and amelioration: AAPG Bulletin, v. 79, p. 1337-1348.

Sotak, J., 2010, Paleoenvironmental changes across the Eocene-Oligocene boundary: insights from the Central-Carpathian Paleogene Basin: Geologica Carpathica, v. 61, p. 393-418.

Suess, E., L. D. Kulm, and J. S. Killingley, 1987, Coastal upwelling and a history of organic-rich mudstone deposition off Peru: Geological Society, London, Special Publications, v. 26, p. 181-197.

Sweeney, J. J., and A. K. Burnham, 1990, Evaluation of a Simple-Model of Vitrinite Reflectance Based on Chemical-Kinetics: AAPG Bulletin, v. 74, p. 1559-1570.

Tegelaar, E., J. De Leeuw, S. Derenne, and C. Largeau, 1989, A reappraisal of kerogen formation: Geochimica et Cosmochimica Acta, v. 53, p. 3103-3106.

ten Haven, H. L., J. W. de Leeuw, J. Rullkötter, and J. S. S. Damsté, 1987, Restricted utility of the pristane/phytane ratio as a palaeoenvironmental indicator: Nature, v. 330, p. 641-643.

Totman Parrish, J., and R. L. Curtis, 1982, Atmospheric circulation, upwelling, and organic-rich rocks in the Mesozoic and Cenozoic eras: Palaeogeography, Palaeoclimatology, Palaeoecology, v. 40, p. 31-66.

Ungerer, P., and R. Pelet, 1987, Extrapolation of the kinetics of oil and gas formation from laboratory experiments to sedimentary basins: Nature, v. 327, p. 52-54.

Van de Meent, D., S. C. Brown, R. P. Philp, and B. R. Simoneit, 1980, Pyrolysis-high resolution gas chromatography and pyrolysis gas chromatography-mass spectrometry of kerogens and kerogen precursors: Geochimica et Cosmochimica Acta, v. 44, p. 999-1013.

van der Boon, A., A. Beniest, A. Ciurej, E. Gaździcka, A. Grothe, R. F. Sachsenhofer, C. G. Langereis, and W. Krijgsman, 2018, The Eocene-Oligocene transition in the North Alpine Foreland Basin and subsequent closure of a Paratethys gateway: Global and Planetary Change, v. 162, p. 101-119.

Vandenbroucke, M., and C. Largeau, 2007, Kerogen origin, evolution and structure: Organic Geochemistry, v. 38, p. 719-833.

Véron, J., 2005, The Alpine Molasse Basin–Review of petroleum geology and remaining potential: Bulletin für Angewandte Geologie, v. 10, p. 75-86.

Vetö, I., 1987, An oligocene sink for organic carbon: Upwelling in the paratethys?: Palaeogeography, Palaeoclimatology, Palaeoecology, v. 60, p. 143-153.

Volkman, J., J. Farrington, R. Gagosian, and S. G. Wakeham, 1981, Lipid composition of coastal marine sediments from the Peru upwelling region: Advances in organic geochemistry, p. 228-240.

Volkman, J. K., S. M. Barrett, and G. A. Dunstan, 1994, C25 and C30 highly branched isoprenoid alkenes in laboratory cultures of two marine diatoms: Organic Geochemistry, v. 21, p. 407-414.

von der Heydt, A., and H. A. Dijkstra, 2006, Effect of ocean gateways on the global ocean circulation in the late Oligocene and early Miocene: Paleoceanography, v. 21, p. n/a-n/a.

Wagner, L. R., 1998, Tectono-stratigraphy and hydrocarbons in the Molasse Foredeep of Salzburg, Upper and Lower Austria: Geological Society, London, Special Publications, v. 134, p. 339-369.

Wakeham, S. G., M. L. Peterson, J. I. Hedges, and C. Lee, 2002, Lipid biomarker fluxes in the Arabian Sea, with a comparison to the equatorial Pacific Ocean: Deep Sea Research Part II: Topical Studies in Oceanography, v. 49, p. 2265-2301.

Widayat, A. H., B. van de Schootbrugge, W. Oschmann, K. Anggayana, and W. Püttmann, 2016, Climatic control on primary productivity changes during development of the Late Eocene Kiliran Jao lake, Central Sumatra Basin, Indonesia: International Journal of Coal Geology, v. 165, p. 133-141.

Yang, S., H.-M. Schulz, N. H. Schovsbo, and J. A. Bojesen-Koefoed, 2017, Oil–source-rock correlation of the Lower Paleozoic petroleum system in the Baltic Basin (northern Europe): AAPG Bulletin, v. 101, p. 1971-1993.

Yang, S. Y., and B. Horsfield, 2016, Some predicted effects of minerals on the generation of petroleum in nature: Energy & Fuels, v. 30, p. 6677-6687.

Zanazzi, A., M. J. Kohn, B. J. MacFadden, and D. O. Terry, 2007, Large temperature drop across the Eocene-Oligocene transition in central North America: Nature, v. 445, p. 639-42.

Ziegler, P., and F. Roure, 1999, Petroleum systems of Alpine-Mediterranean foldbelts and basins: Geological Society, London, Special Publications, v. 156, p. 517-540.

Samples	Depth (m)	LECO combustion and Rock-Eval								PyGC								Bulk kinetic	GC-FID	GC-MS									
		TOC (%)*	TOC/S*	TIC	Carb (%)	S1 (mg/g)	S2 (mg/g)	Tmax (°C)*	HI (mg/g TOC)*	C1-5 Bulk*	nC6-14 Res.	nC15+ Res.	2,3-dmThiophene	n-nonene; 9:1	o-xylene	o-Xyl/C_9*	2,3-dMT/C9*	GeoTmax (°C)*	Pr/Ph*	C25HBI/C21*	OL/(OL+H)*	C31H/C30H*	C35H/C34H*	St/H*	St 27*	St 28*	St 29	MTTC ratio*	OL index*MTTC
Dynow 1	1378.6	1.5	1.9	5.84	48.7	0.1	7.03	430	468.7	74.00%	18.50%	7.50%	11.40%	44.40%	44.10%	0.99	0.26	153	2.93	0	0.11	0.49	0.75	0.93	26.40%	38.50%	35.10%	0.82	0.092
Dynow 2	1380.3	0.52	1.81	9.98	83.2	0.02	2.19	430	420.2	73.70%	19.80%	6.50%	10.70%	44.20%	45.00%	1.02	0.24	154	2.15	0	0.1	0.39	0.97	1.18	20.40%	45.80%	33.80%	0.98	0.096
Dynow 3	1380.6	1.84	2.02	7.12	59.3	0.12	9.85	428	535.1	70.00%	19.80%	10.10%	11.60%	49.00%	39.40%	0.8	0.24	153	2.18	0	0.14	0.4	1.03	1.04	23.20%	40.50%	36.30%	0.72	0.1
Dynow 4	1382.4	1.92	4.68	10.47	87.2	0.17	9.2	426	479	70.40%	20.00%	9.60%	10.90%	47.30%	41.80%	0.88	0.23	151	2.35	0	0.11	0.44	1.01	0.76	25.70%	38.40%	35.90%	0.75	0.083
U.Schöneck 1	1382.7	7.75	2.52	0.29	2.4	1.08	42.34	420	546.3	62.00%	22.50%	15.50%	12.60%	54.70%	32.70%	0.6	0.23	148	1.12	0.58	0.09	0.64	1.51	0.7	35.00%	30.00%	35.00%	0.57	0.053
U.Schöneck 2	1384.7	4.95	0.9	0.1	0.8	1.12	29.8	423	602.1	58.00%	26.00%	16.00%	11.60%	57.40%	31.00%	0.54	0.21	147	1.62	0.51	0.06	0.67	1.74	0.68	32.40%	34.50%	33.10%	0.61	0.039
U.Schöneck 3	1385.8	7.34	2.05	0.08	0.7	1.02	42.5	421	579	60.40%	25.70%	13.90%	11.60%	56.80%	31.60%	0.56	0.2	149	1.13	0.52	0.08	0.65	1.61	0.65	33.50%	30.70%	35.80%	0.59	0.048
L.Schöneck 1	1389.4	2.56	1.19	5.5	45.8	0.17	12.33	412	481.6	75.00%	18.70%	6.30%	23.70%	34.80%	41.50%	1.19	0.68	143	1.22	0.41	0.24	0.63	2.21	2.23	39.10%	28.10%	32.80%	0.63	0.153
L.Schöneck 2	1391.7	1.77	0.67	1.66	13.8	0.14	6.82	411	385.2	75.20%	17.80%	7.00%	31.30%	36.00%	32.70%	0.91	0.87	134	1.91	0.34	0.2	0.59	1.86	1.65	38.40%	27.30%	34.30%	0.87	0.176
L.Schöneck 3	1393.4	2.05	0.93	0.21	1.7	0.09	7.23	410	352.7	79.70%	16.90%	3.50%	25.00%	32.90%	42.10%	1.28	0.76	136	2.2	0.36	0.3	0.73	2.15	2.15	37.70%	27.70%	34.70%	0.79	0.238

1

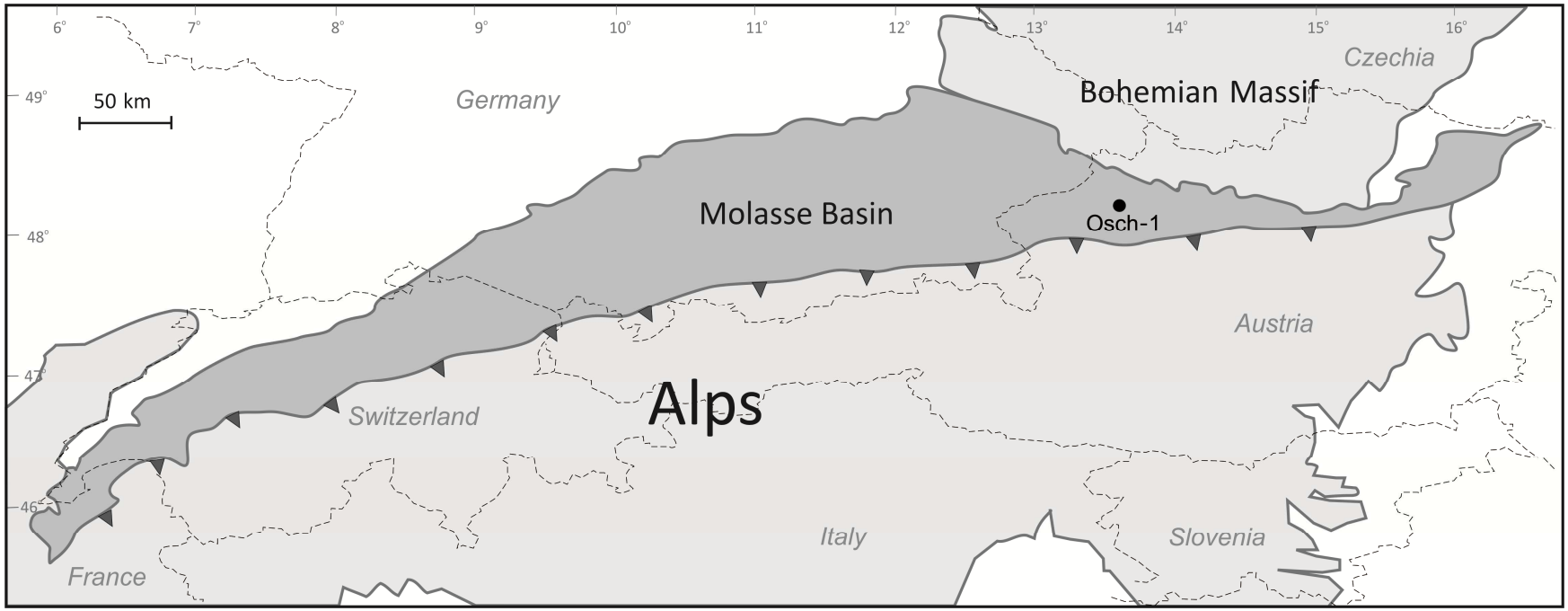
6°
7°
8°
9°
10°
11°
12°
13°
14°
15°
16°
49°
48°
47°
46°
50 km
Germany
Czechia
Bohemian Massif
Molasse Basin
Osch-1
Austria
Switzerland
Alps
Italy
Slovenia
France

2

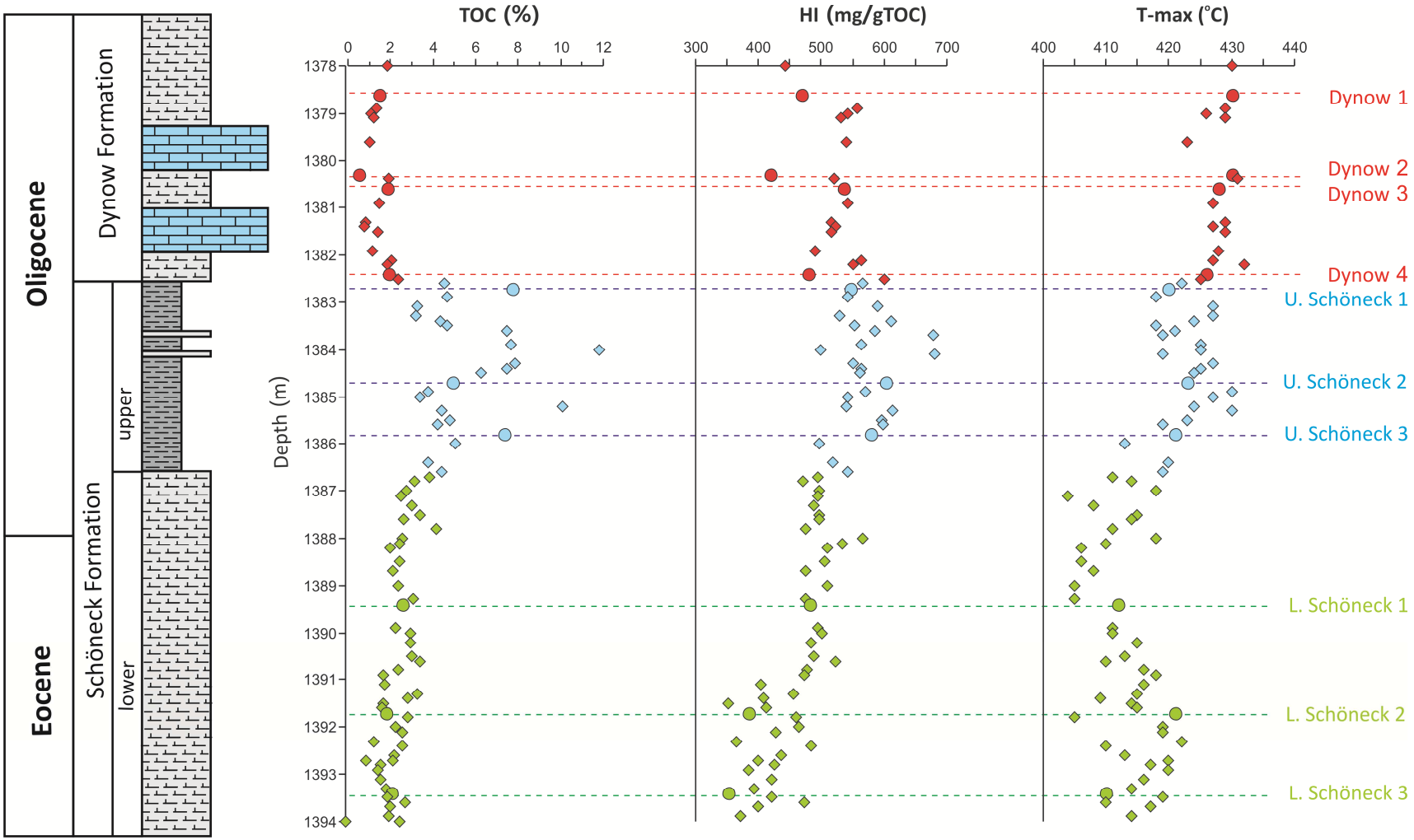
Oligocene
Eocene
Dynow Formation
Schöneck Formation
upper
lower
TOC (%)
0
2
4
6
8
10
12
HI (mg/gTOC)
300
400
500
600
700
T-max (°C)
400
410
420
430
440
Depth (m)
1378
1379
1380
1381
1382
1383
1384
1385
1386
1387
1388
1389
1390
1391
1392
1393
1394
Dynow 1
Dynow 2
Dynow 3
Dynow 4
U. Schöneck 1
U. Schöneck 2
U. Schöneck 3
L. Schöneck 1
L. Schöneck 2
L. Schöneck 3

3

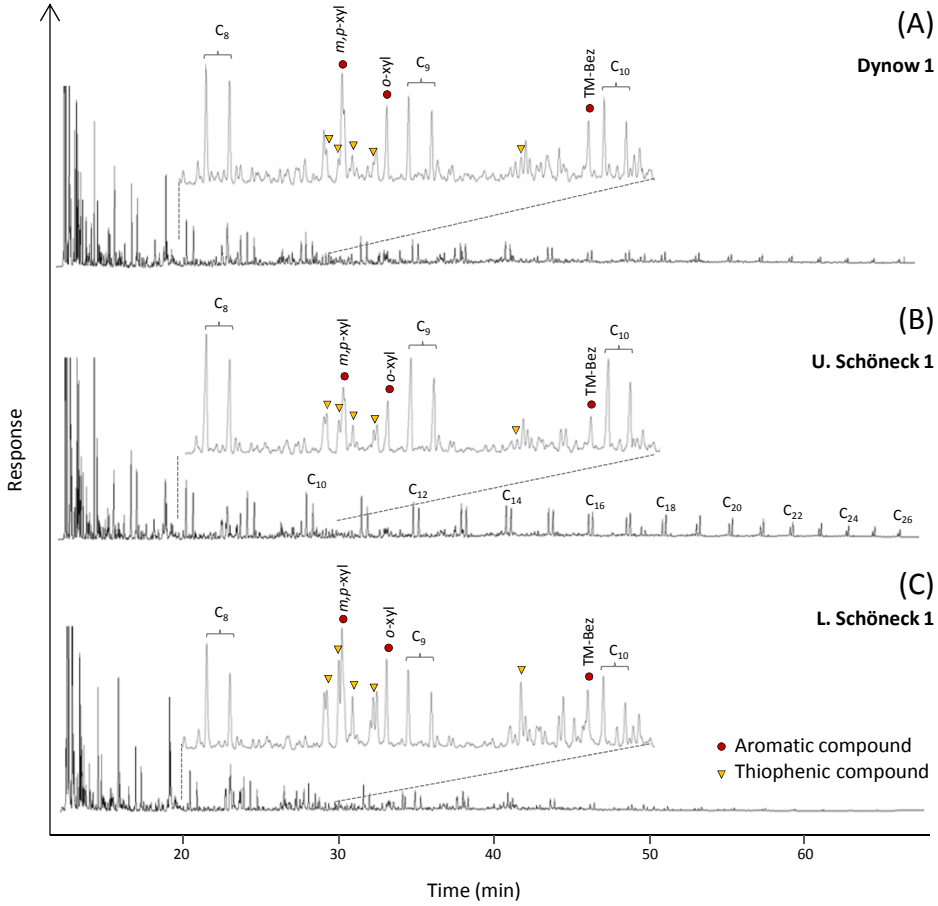
(A)
Dynow 1
(B)
U. Schöneck 1
(C)
L. Schöneck 1
C8
m,p-xyl
o-xyl
C9
TM-Bez
C10
C12
C14
C16
C18
C20
C22
C24
C26
Aromatic compound
Thiophenic compound
Response
20
30
40
50
60
Time (min)

4

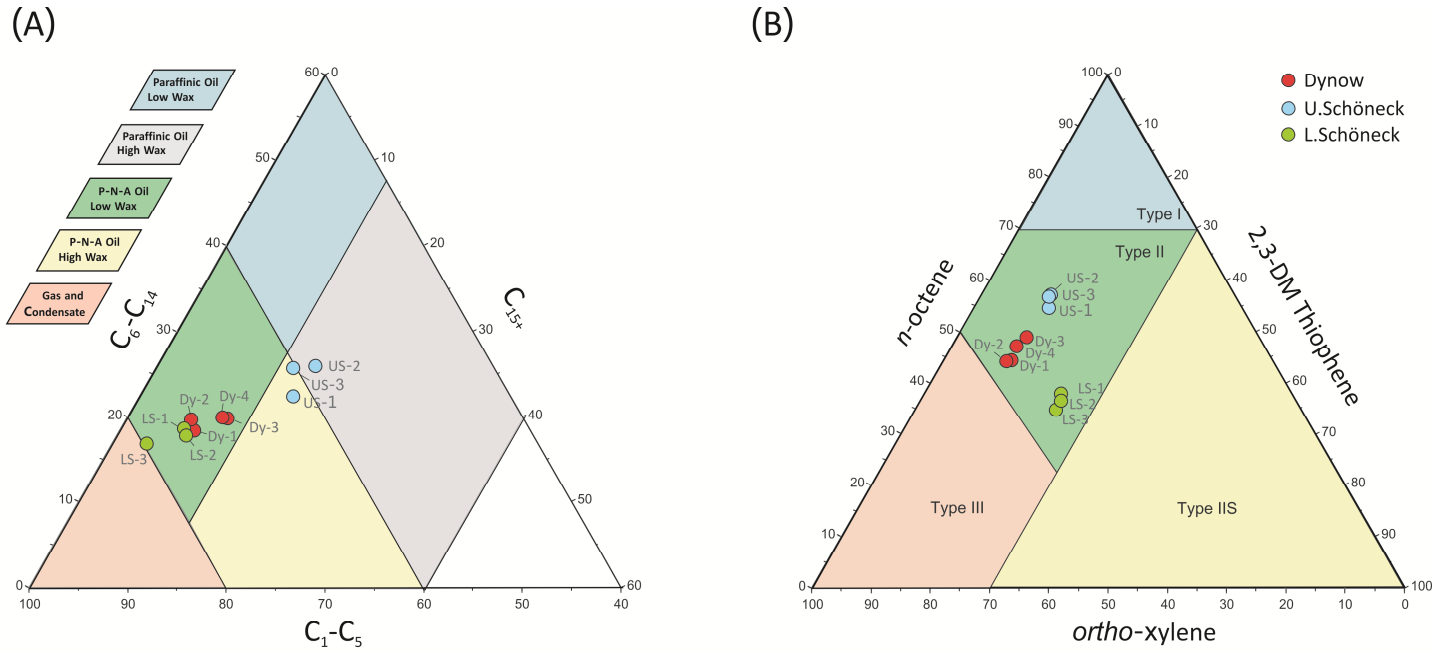
(A)
Paraffinic Oil Low Wax
Paraffinic Oil High Wax
P-N-A Oil Low Wax
P-N-A Oil High Wax
Gas and Condensate
C6-C14
C15+
C1-C5
US-2
US-3
US-1
Dy-2
Dy-4
Dy-3
Dy-1
LS-1
LS-2
LS-3
(B)
Dynow
U.Schöneck
L.Schöneck
Type I
Type II
Type III
Type IIS
n-octene
2,3-DM Thiophene
ortho-xylene

5

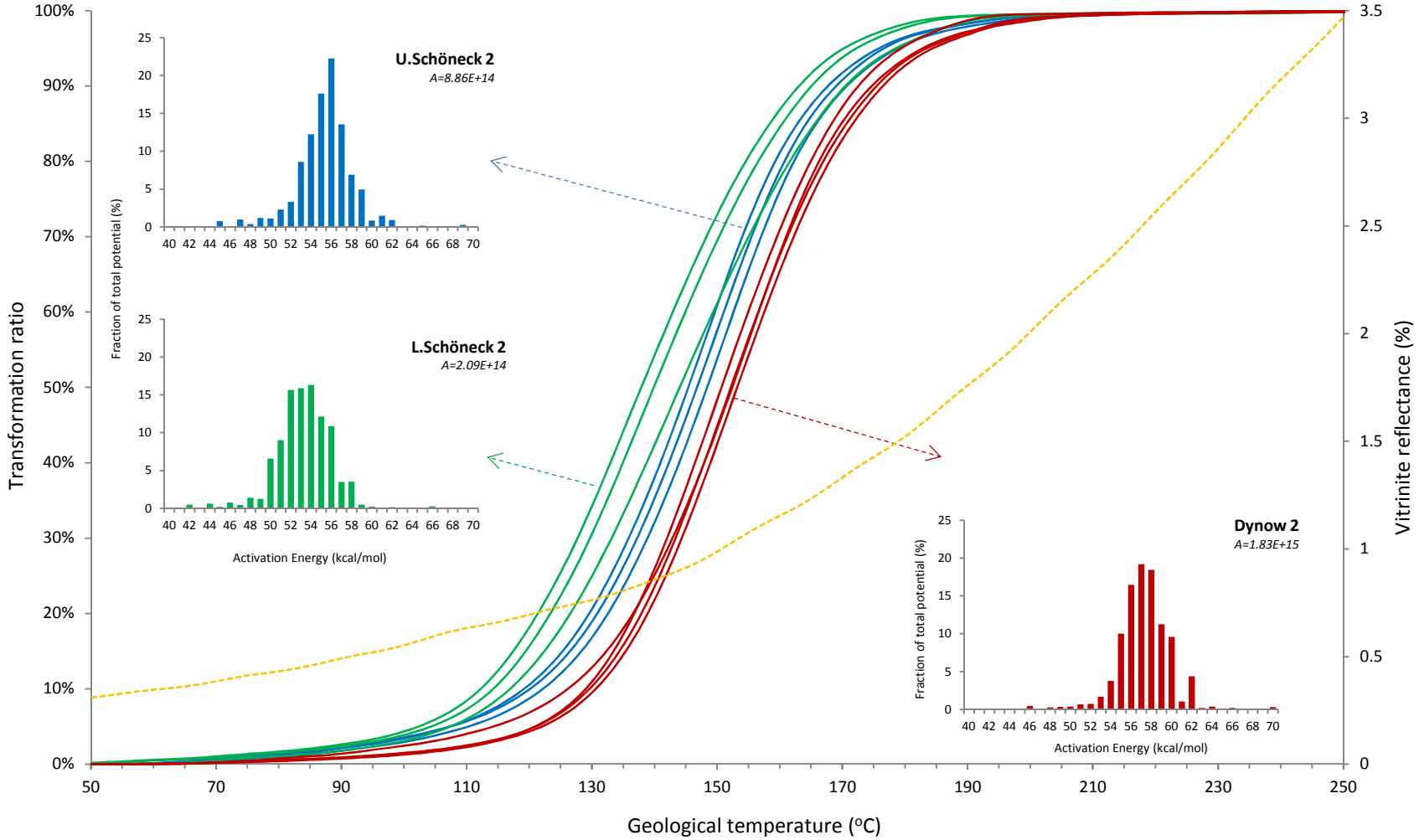
Transformation ratio
Vitrinite reflectance (%)
Geological temperature (°C)
U.Schöneck 2
A=8.86E+14
L.Schöneck 2
A=2.09E+14
Dynow 2
A=1.83E+15
Fraction of total potential (%)
Activation Energy (kcal/mol)

6 **TIC**

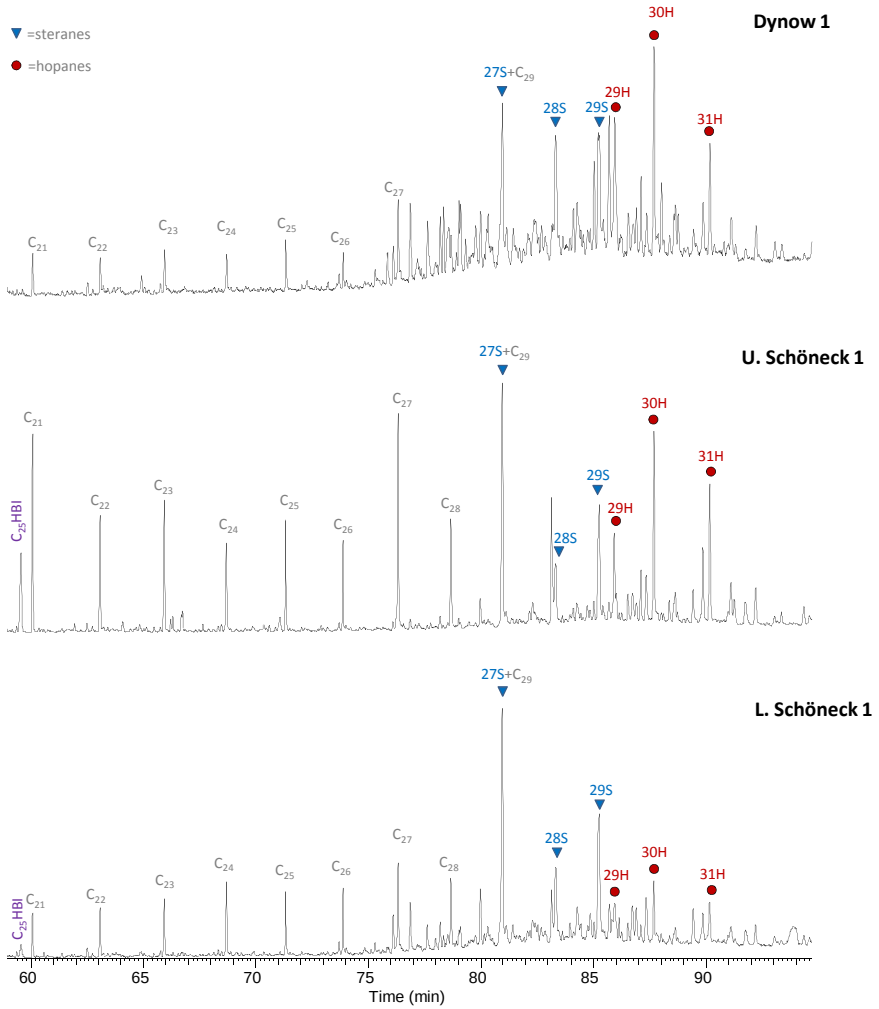
=steranes
=hopanes
Dynow 1
U. Schöneck 1
L. Schöneck 1
C21
C22
C23
C24
C25
C26
C27
C28
C25HBI
27S+C29
28S
29S
29H
30H
31H
60
65
70
75
80
85
90
Time (min)

7

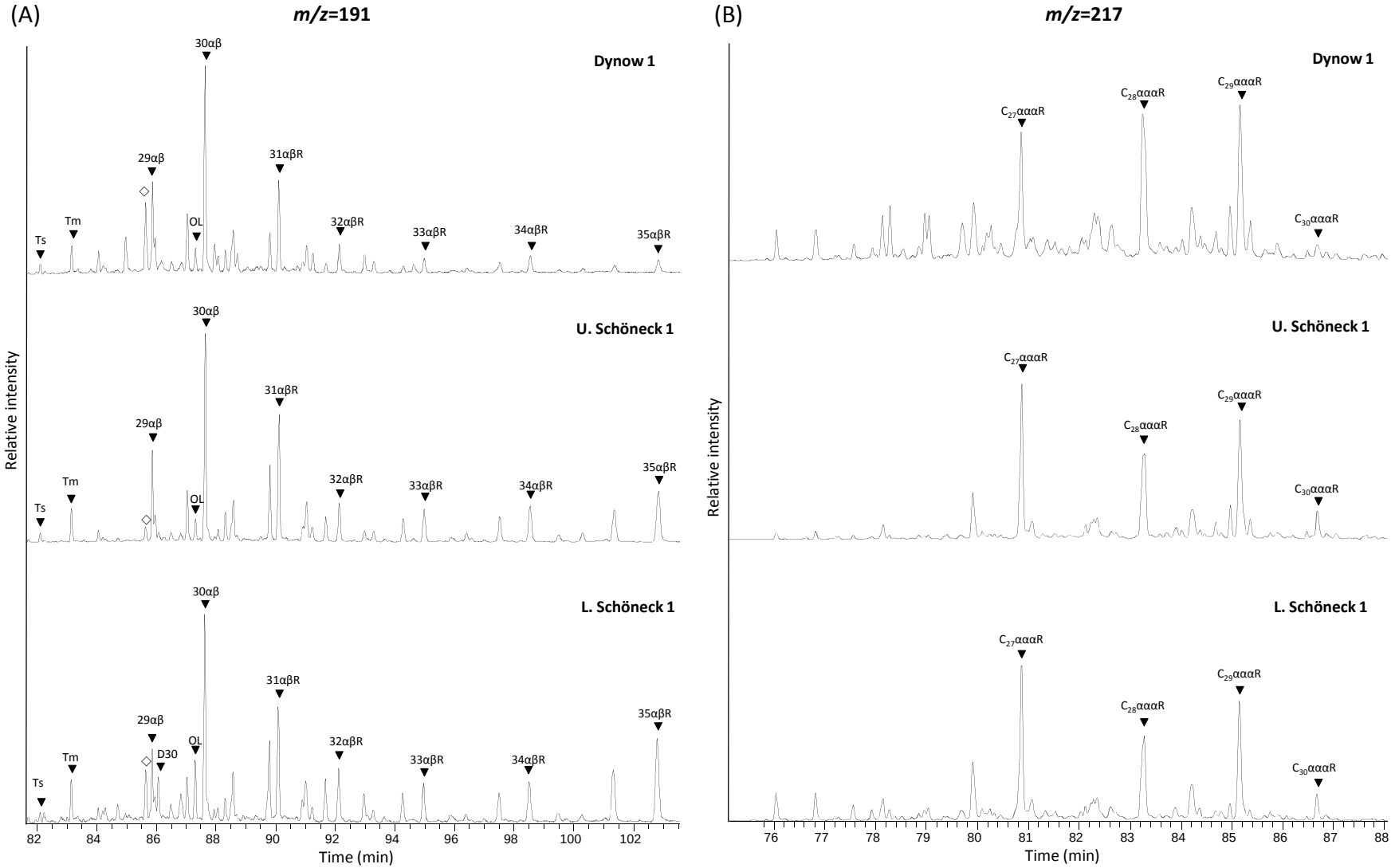
(A)
m/z=191
Dynow 1
U. Schöneck 1
L. Schöneck 1
Ts
Tm
29αβ
30αβ
OL
31αβR
32αβR
33αβR
34αβR
35αβR
D30
Relative intensity
Time (min)
(B)
m/z=217
C27αααR
C28αααR
C29αααR
C30αααR

8

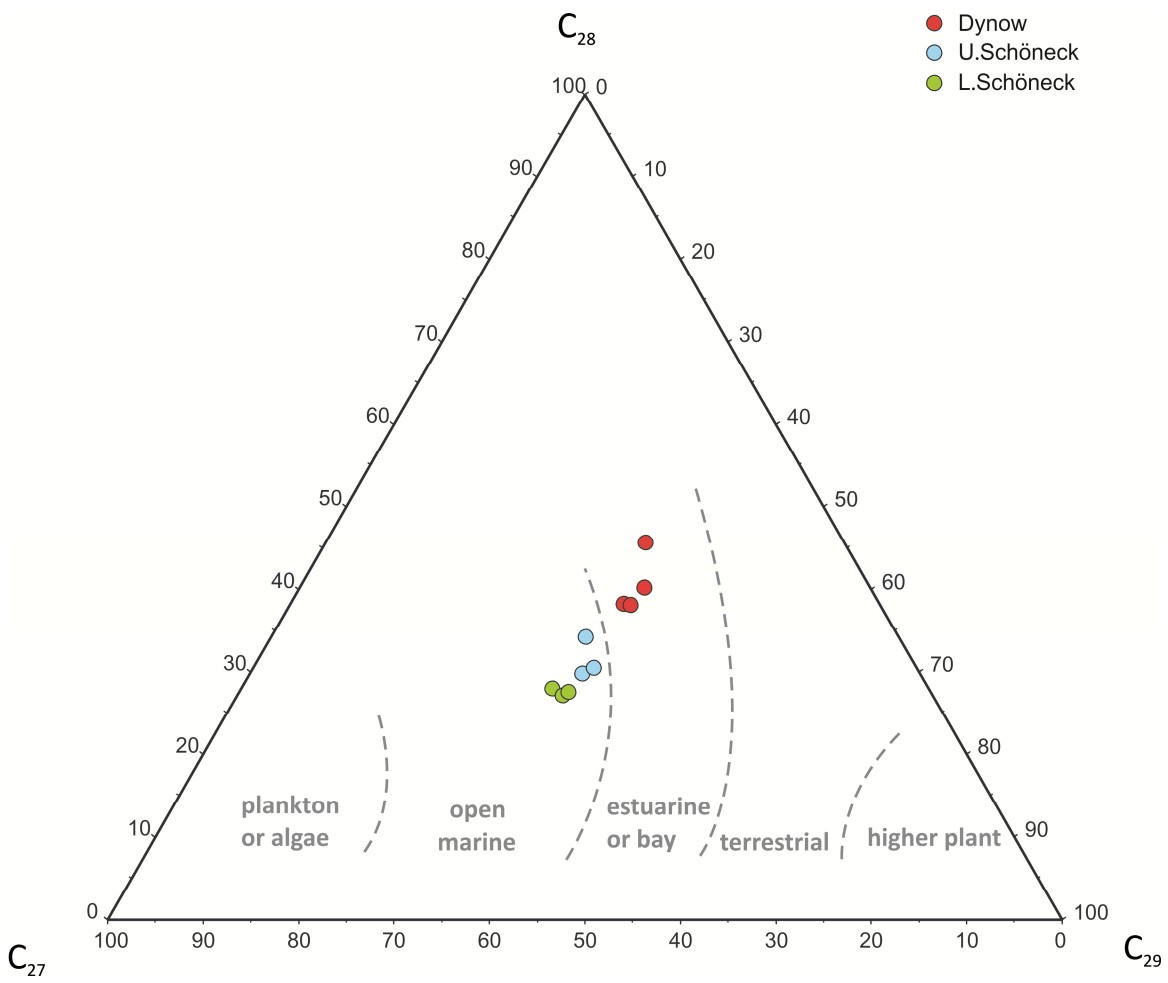
C28
C27
C29
Dynow
U.Schöneck
L.Schöneck
plankton or algae
open marine
estuarine or bay
terrestrial
higher plant

9

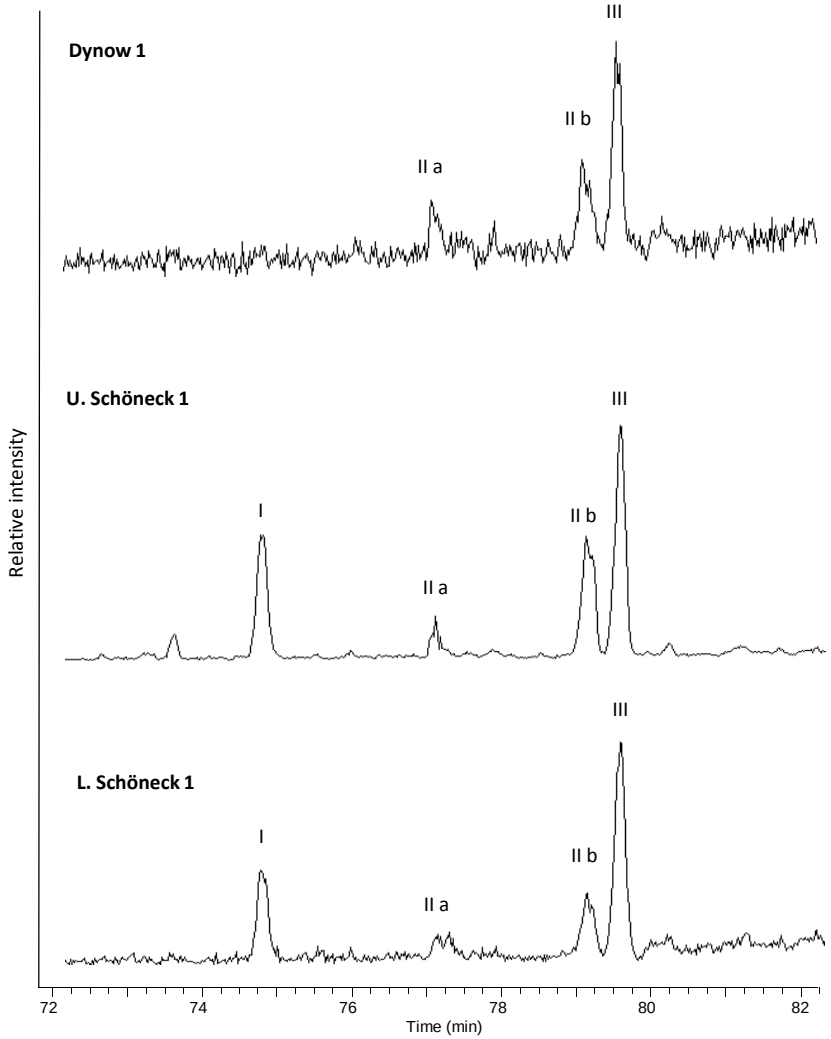
Dynow 1
III
II b
II a
U. Schöneck 1
III
I
II b
II a
L. Schöneck 1
III
I
II b
II a
Relative intensity
72
74
76
78
80
82
Time (min)

10

(A)

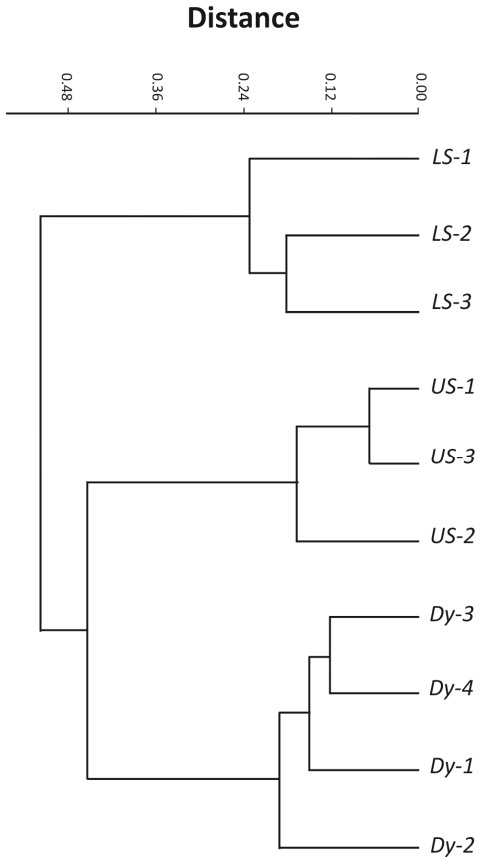
Distance
0.48
0.36
0.24
0.12
0.00
LS-1
LS-2
LS-3
US-1
US-3
US-2
Dy-3
Dy-4
Dy-1
Dy-2

(B)

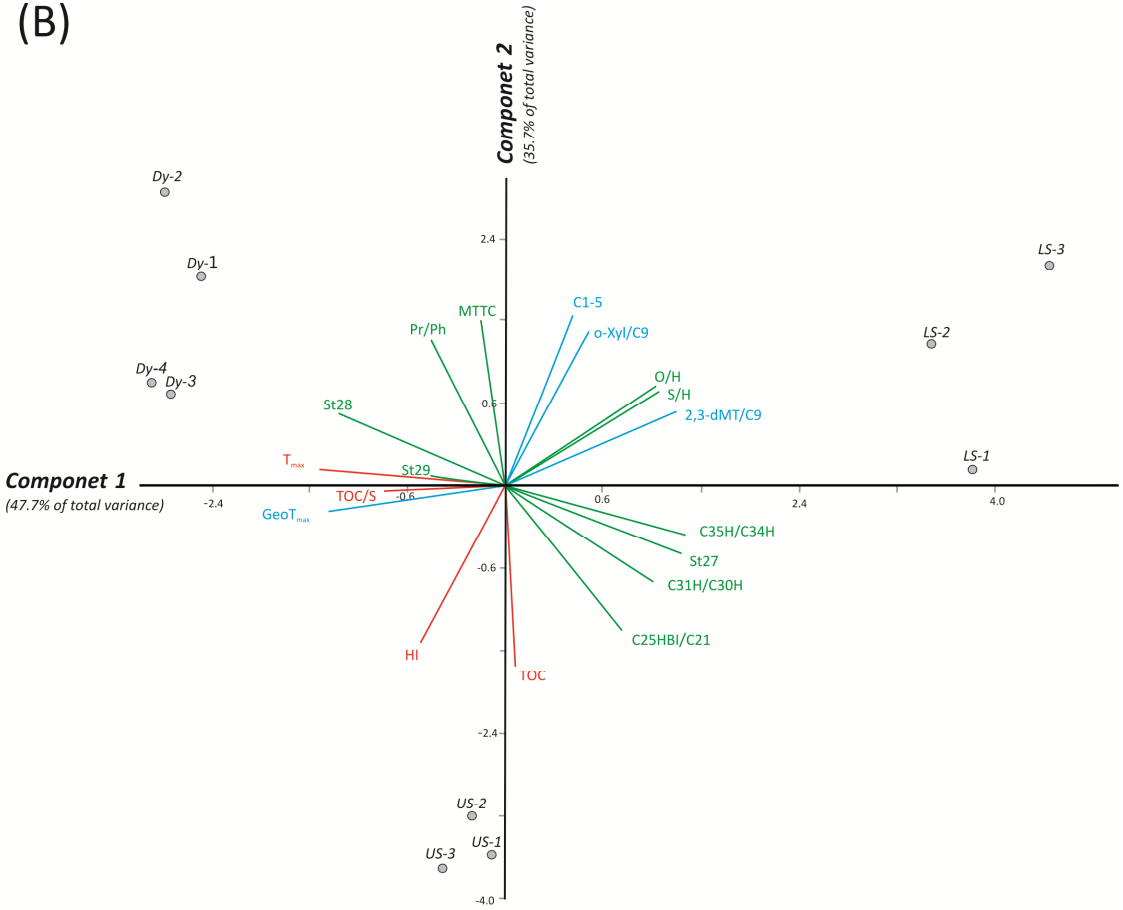
Componet 2
(35.7% of total variance)
Componet 1
(47.7% of total variance)
Dy-2
Dy-1
Dy-4
Dy-3
LS-3
LS-2
LS-1
US-2
US-1
US-3
MTTC
C1-5
Pr/Ph
o-Xyl/C9
O/H
S/H
2,3-dMT/C9
St28
T max
St29
TOC/S
GeoT max
C35H/C34H
St27
C31H/C30H
C25HBI/C21
HI
TOC
2.4
0.6
-2.4
-0.6
-4.0
4.0

11

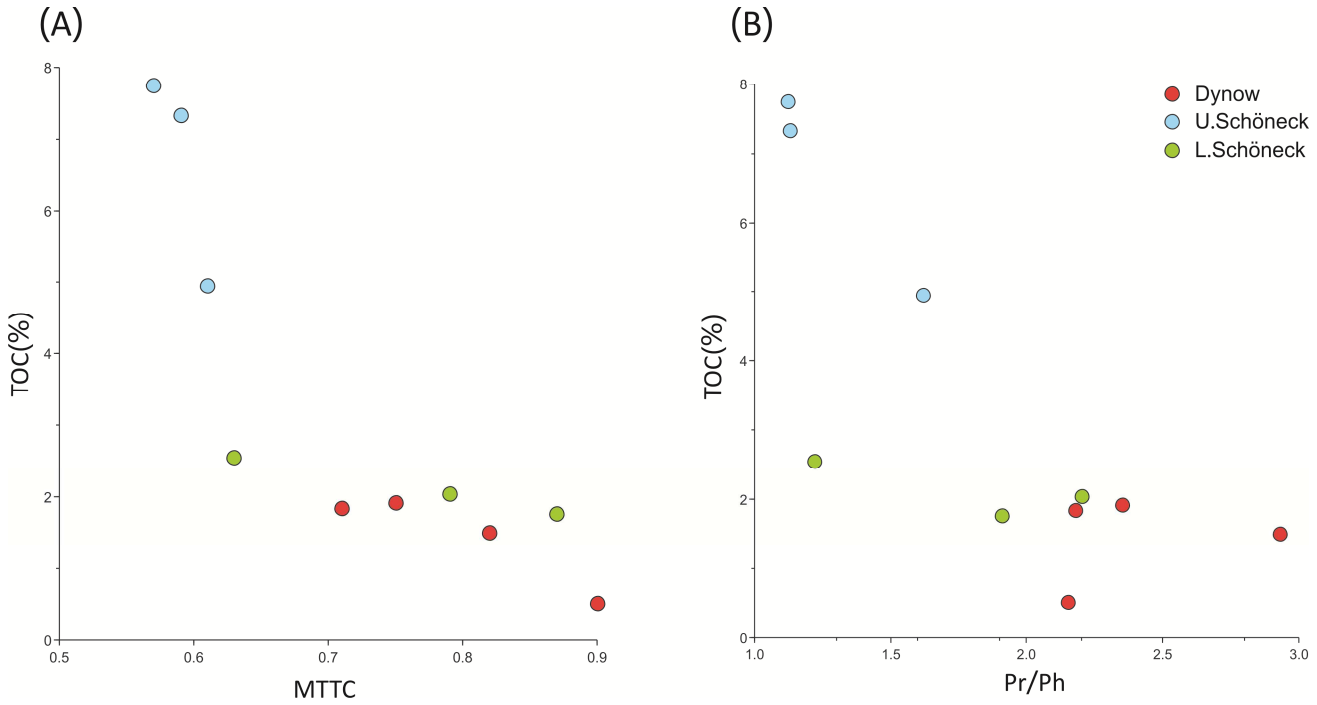
(A)
TOC(%)
MTTC
0
2
4
6
8
0.5
0.6
0.7
0.8
0.9
(B)
TOC(%)
Pr/Ph
1.0
1.5
2.0
2.5
3.0
Dynow
U.Schöneck
L.Schöneck

12

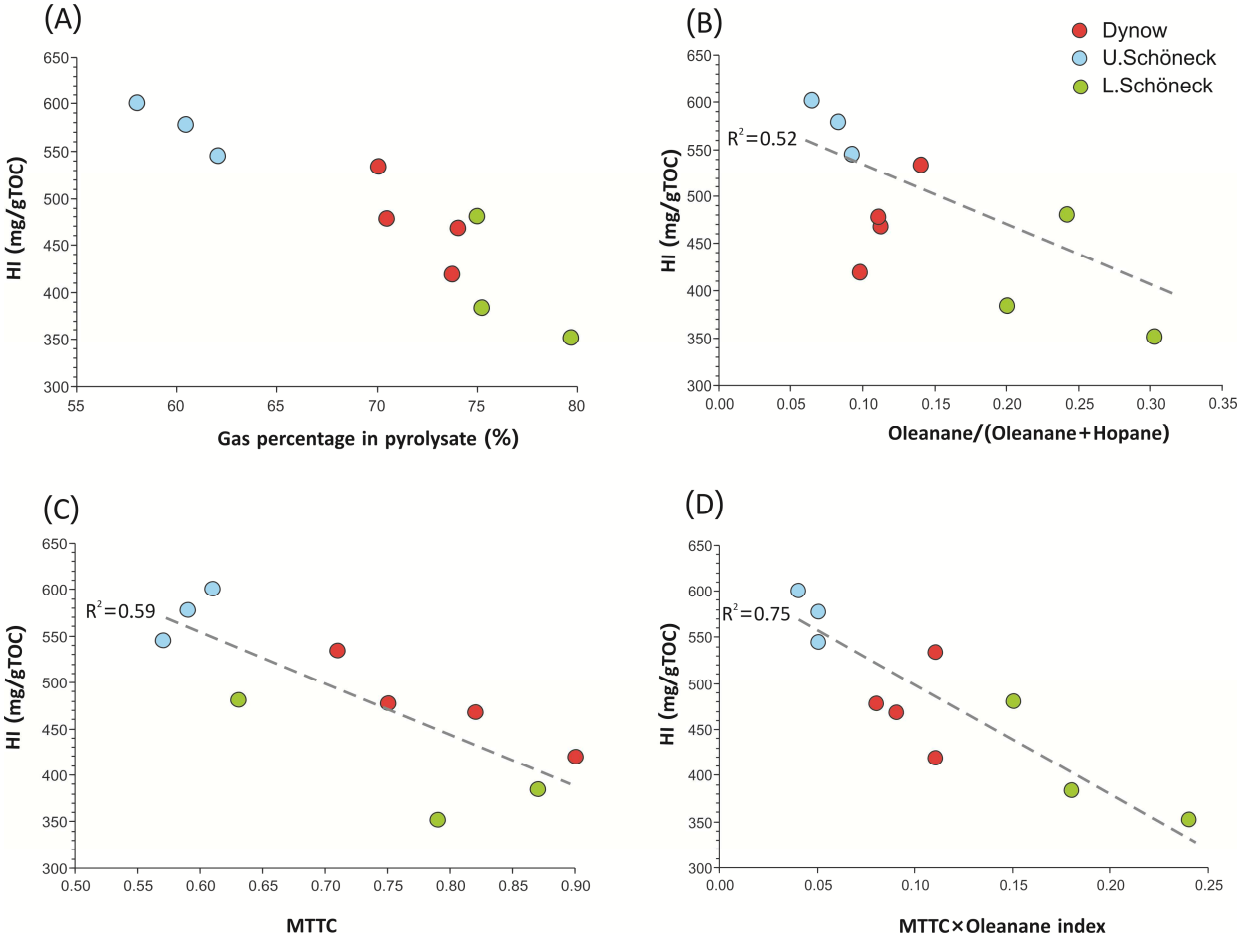
(A)
HI (mg/gTOC)
650
600
550
500
450
400
350
300
55
60
65
70
75
80
Gas percentage in pyrolysate (%)
(B)
Dynow
U.Schöneck
L.Schöneck
R²=0.52
HI (mg/gTOC)
0.00
0.05
0.10
0.15
0.20
0.25
0.30
0.35
Oleanane/(Oleanane+Hopane)
(C)
R²=0.59
HI (mg/gTOC)
0.50
0.55
0.60
0.65
0.70
0.75
0.80
0.85
0.90
MTTC
(D)
R²=0.75
HI (mg/gTOC)
0.00
0.05
0.10
0.15
0.20
0.25
MTTC×Oleanane index

13

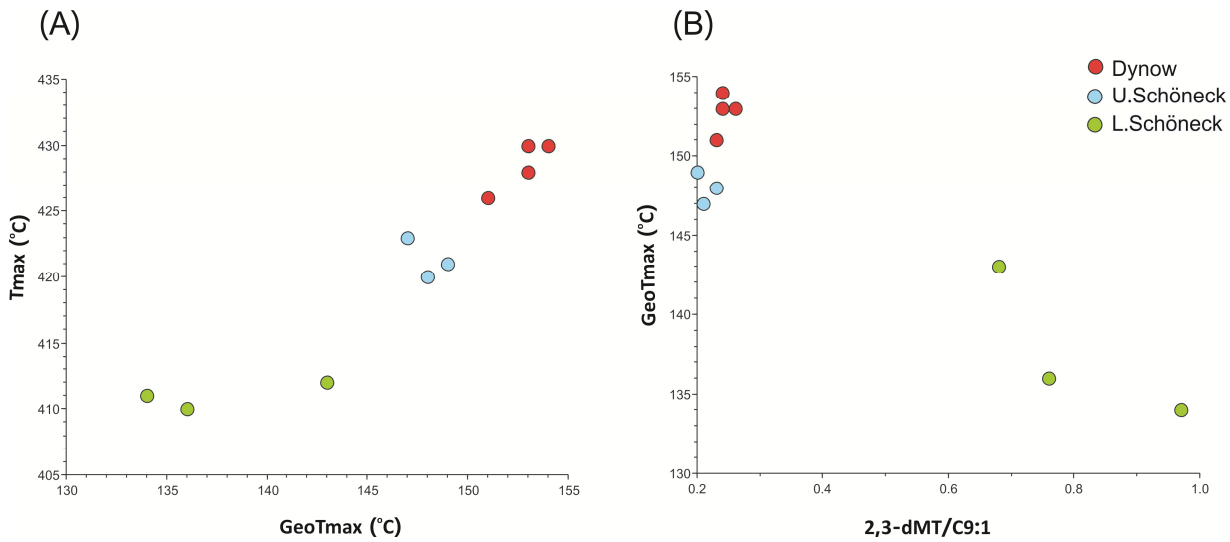
(A)
Tmax (°C)
GeoTmax (°C)
435
430
425
420
415
410
405
130
135
140
145
150
155
(B)
GeoTmax (°C)
2,3-dMT/C9:1
155
150
145
140
135
130
0.2
0.4
0.6
0.8
1.0
Dynow
U.Schöneck
L.Schöneck

- Biplots can point out the controlling factors of petroleum generation potentials.
- The product of MTTC and OL index controls the HI.
- Lower T_{max} values are induced by higher organic sulphur contents.
- Global glaciation might promote the development of petroleum source rocks.